Eur Biophys J (2006) 35: 477–493
DOI 10.1007/s00249-006-0055-9

ARTICLE

M. A. Kiselev · E. V. Zemlyanaya · V. K. Aswal
R. H. H. Neubert

What can we learn about the lipid vesicle structure from the small-angle neutron scattering experiment?

Received: 23 August 2005 / Revised: 3 February 2006 / Accepted: 14 March 2006 / Published online: 14 April 2006

Abstract Small-angle neutron scattering (SANS) on the unilamellar vesicle (ULV) populations (diameter 500 and 1,000 Å) in D_2O was used to characterize lipid vesicles from dimyristoylphosphatidylcholine (DMPC) at three phases: gel $L_{\beta'}$, ripple $P_{\beta'}$ and liquid L_α. Parameters of vesicle populations and internal structure of the DMPC bilayer were characterized on the basis of the separated form factor (SFF) model. Vesicle shape changes from nearly spherical in the L_α phase to elliptical in the $P_{\beta'}$ and $L_{\beta'}$ phases. This is true for vesicles prepared via extrusion through pores with the diameter 500 Å. Parameters of the internal bilayer structure (thickness of the membrane and the hydrophobic core, hydration and the surface area of the lipid molecule) were determined on the basis of the hydrophobic–hydrophilic (HH) approximation of neutron scattering length density across the bilayer $\rho(x)$ and of the step function (SF) approximation of $\rho(x)$. DMPC membrane thickness in the L_α phase ($T = 30$°C) demonstrates a dependence on the membrane curvature for extruded vesicles. Prepared via extrusion through 500 Å diameter pores, vesicle population in the L_α phase has the following characteristics: average value of minor semi-axis 266 ± 2 Å, ellipse eccentricity 1.11 ± 0.02, polydispersity 26%, thickness of the membrane 48.9 ± 0.2 Å and of the hydrophobic core 19.9 ± 0.4 Å, surface area 60.7 ± 0.5 Å^2 and number of water molecules 12.8 ± 0.3 per DMPC molecule. Vesicles prepared via extrusion through pores with the diameter 1,000 Å have polydispersity of 48% and membrane thickness of 45.5 ± 0.6 Å in the L_α phase. SF approximation was used to describe the DMPC membrane structure in $L_{\beta'}$ ($T = 10$°C) and $P_{\beta'}$ ($T = 20$°C) phases. Extruded DMPC vesicles in D_2O have membrane thickness of 49.6 ± 0.5 Å in the $L_{\beta'}$ phase and 48.3 ± 0.6 Å in the $P_{\beta'}$ phase. The dependence of the DMPC membrane thickness on temperature was restored from the SANS experiment.

Keywords Phospholipids · Lipid membrane · Vesicles · Small-angle neutron scattering

Abbreviations DMPC: Dimyristoylphosphatidylcholine · DPPC: Dipalmitoylphosphatidylcholine · DSPC: Distearoylphosphatidylcholine · DHPC: Dihexadecylphosphatidylcholine · POPC: Palmitoyloleoylphosphatidylcholine · SANS: Small-angle neutron scattering · SAXS: Small-angle X-ray scattering · SF: Step function · HH: Hydrophobic–hydrophilic · SFF: Separated form factor · HS: Hollow sphere · ULVs: Unilamellar vesicles · MLVs: Multilamellar vesicles · DSC: Differential scanning calorimetry · $L_{\beta'}$: Gel phase · $P_{\beta'}$: Ripple phase · L_α: Liquid crystalline phase

M. A. Kiselev (✉)
Frank Laboratory of Neutron Physics,
Joint Institute for Nuclear Research,
Dubna 141980 Moscow Region, Russia
E-mail: Kiselev@jinr.ru
Tel.: +7-096-2166977
Fax: +7-096-2165484

E. V. Zemlyanaya
Laboratory of Information Technologies,
Joint Institute for Nuclear Research,
Dubna 141980 Moscow Region, Russia

V. K. Aswal
Solid State Physics Division,
Bhabha Atomic Research Centre, Trombay,
Mumbai 400 085, India

R. H. H. Neubert
Institute of Pharmaceutical Technology and Biopharmacy,
Martin-Luther-University, Halle (Saale) 06120, Germany

Introduction

Phospholipids are the main components of cell membranes. Research into the structure of phospholipids is important from the viewpoint of structural biology and biochemistry. Unilamellar vesicles (ULVs) are especially interesting because most biological membranes are unilamellar and the function and properties of integral

membrane proteins depend on the lipid bilayer structure. ULVs are also used as delivery agents for drugs. Knowledge of their structure at nanoscale is important for pharmacology (Nagayasu et al. 1999; Cevc et al. 2002).

Dynamic and static light scattering are commonly used to characterize the form and size of vesicles. However, these methods have the limitation of obtaining information about the thickness and the internal structure of the membrane bilayer (Pencer et al. 2001; Jin et al. 1999). Most of the knowledge about the internal structure of phospholipids in L_α and $L_{\beta'}$ phases was obtained by X-ray diffraction on giant multilamellar vesicles (MLVs) in H_2O, which have negligibly small membrane curvature (Nagle and Tristram-Nagle 2000). In many works, small-angle neutron scattering (SANS) has been used to characterize the bilayer structure of ULVs at high excess of D_2O. Membrane thickness can be found by experimentally measuring the radius of gyration of the bilayer using the Guinier approximation (Feigin and Svergun 1987; Knoll et al. 1981; Gordeliy et al. 1993, 2005; Balgavy et al. 1998). Calculations of bilayer parameters from the radius of gyration are based on the part of SANS curve in the interval of scattering vector q from 0.03 to 0.14 Å^{-1}. This approach was used to calculate the bilayer thickness and lipid surface area of the DMPC membrane in L_α phase on the basis of strip function model of the neutron scattering length density (Kucerka et al. 2004b). The electron density profile or the one of neutron scattering length density is calculated by Fourier transformation from diffraction peak intensities in the diffraction experiment on the MLVs or oriented dry membranes (Wiener and White 1991; Nagle and Tristram-Nagle 2000; Tristram-Nagle et al. 2002). An accuracy of the determination of structure depends on the space resolution of the scattering experiment:

$$\Delta x \approx \frac{\pi}{q_m}, \tag{1}$$

where q_m is a maximum value of the measured scattering vector. In the diffraction experiment,

$$\frac{\pi}{q_m} \approx 0.5 \frac{d_u}{h_m}, \tag{2}$$

where d_u is the repeat distance and h_m the maximum diffraction order. In excess water, the DMPC membrane has $d_u = 62.7$ Å at $T = 30°C$ and $\Delta x = 3.9$ Å for $h_m = 8$. In SANS experiment, a coherent scattering intensity of vesicle population can be measured to $q_m \approx 0.3$ Å^{-1}. This gives a resolution $\Delta x = 10.5$ Å of the Fourier transformation, which limits an application of the indirect Fourier transformation for the evaluation of the internal membrane structure from SANS experiment (Glatter 1977, 1980).

Small-angle X-ray scattering (SAXS) has smaller value of the incoherent background relative to SANS, which allows one to measure the coherent SAXS scattering from bilayer form factor up to the value of $q = 0.4$ Å^{-1} and improves the resolution of the Fourier transformation to the value $\Delta x = 7.9$ Å (Kiselev et al. 2005a; Kucerka et al. 2005). The disadvantage of the SAXS application for the ULVs characterization is a low value of the contrast $\Delta\rho$ between the membrane and water. The X-ray contrast between DMPC molecules in the L_α phase and water is $|\Delta\rho_x| = 0.14 \times 10^{10}$ cm^{-2}. In the case of neutron scattering, the contrast is $|\Delta\rho_n| = 0.45 \times 10^{10}$ cm^{-2}, whereas the application of D_2O increases the neutron contrast to $|\Delta\rho_n| = 5.6 \times 10^{10}$ cm^{-2}. For vesicles in water, the form factor of vesicle size is complex to be measured without contrast improvement. Disaccharide solutions in water were used to improve the contrast conditions in SAXS experiment on the DMPC vesicles: 40% sucrose solution (w/w) increases the X-ray contrast by a factor of 10 compared to that of pure H_2O (Kiselev et al. 2001, 2003b). The surfactant ($C_7F_{15}COOLi$) with fluorinated chains was used for the X-ray contrast improvement in the investigation of ULVs formation by rapid mixing of the anionic and zwitterionic micelles (Weiss et al. 2005).

Design of appropriate scattering models and approximations of the scattering length density along the normal to the bilayer $\rho(x)$ (based on some preliminary knowledge about bilayer structure) could improve the spatial resolution in an evaluation of the internal membrane structure from SANS experiment. The model of randomly oriented planar bilayer was applied for identification of the membrane thickness and internal membrane structure (Pencer and Hallet 2000; Kucerka et al. 2004b). Step function (SF) approximation of $\rho(x)$ was applied for the investigation of oligolamellar vesicles (Schmiedel et al. 2001). This approach could be used to obtain additional information about the membrane repeat distance and percentage of non-ULVs (Schmiedel et al. 2005). Other important information about vesicle population concerns the average vesicle radius and polydispersity. The hollow sphere (HS) model was applied for the calculation of vesicle radius, vesicle polydispersity, membrane thickness and internal membrane structure (Kiselev et al. 2001; Balgavy et al. 2001). The application of the HS model allows the possibility to describe the internal membrane structure as two or three regions with constant scattering length density via SF approximation of $\rho(x)$. The HS model has two principal drawbacks: (a) it can only be used for spherical vesicles, (b) $\rho(x)$ can only be described as a step function, whereas neutron diffraction experiments demonstrate that $\rho(x)$ has a more complex and smooth shape (Wiener and White 1991; Gordeliy and Kiselev 1995).

A model of separated form factors (SFF) allows simulation of $\rho(x)$, using almost any function, which significantly expands the possibilities of studying the internal membrane structure (Kiselev et al. 2002). The size of DMPC vesicle does not depend sufficiently on the different functions used for modeling $\rho(x)$. However, the values of membrane thickness d, thickness of the hydrophobic region D and the number of water molecule within a bilayer per DMPC molecule N_w are

sensitive to the type of function $\rho(x)$ (Kiselev et al. 2004; Kucerka et al. 2004b).

In the case of homogeneous approximation, $\rho(x) = \text{const}$, D_2O penetration into the bilayer makes part of the hydrophilic region invisible relative to the bulk D_2O (Kiselev et al. 2004). Therefore, approximation of $\rho(x) = \text{const}$ gives an underestimated value of $d = 35.2 \pm 0.2$ Å for DMPC vesicles at $T = 30$°C (Kiselev et al. 2003b). The result, based on the SF approximation of $\rho(x)$, is more reasonable: $d = 44.5 \pm 0.3$ Å (Kucerka et al. 2004b). Generation of $\rho(x)$ based on the Gaussian functions gives $d = 50.6 \pm 0.8$ Å (Kiselev et al. 2004). The water distribution function across the bilayer has sigmoidal form (Armen et al. 1998; Kiselev et al. 2004). In liquid L_α phase, the contribution from the D_2O distribution function to the integrated neutron scattering length density of DMPC is sufficiently larger than the one from the polar head group (Kiselev et al. 2004). Competition between contributions of D_2O and polar head groups to the integrated neutron scattering length density allows one to simplify the approximation of $\rho(x)$ and decrease the number of fit parameters.

It is commonly believed that contrast variation (variation of the H_2O/D_2O ratio in the water) can improve the validity of obtained parameters in SANS experiment. This is true when penetration of water inside the studied object is negligibly small and $\rho(x)$ can be considered as constant or step function with parameters, which are independent of the scattering length density of H_2O/D_2O solvent. For example, the application of the contrast variation for evaluation of the DMPC membrane thickness in L_α phase gives membrane thickness 32 Å for the $\rho(x) = \text{const}$ and 37 ± 4 Å for more realistic approximation of the $\rho(x)$ (Kucerka et al. 2004a). Both the values obtained from contrast variation should be considered as thickness parameter of the "dry" membrane. It was shown that the best condition for the evaluation of the membrane thickness is infinite contrast (Gordeliy et al. 1993; Kucerka et al. 2004a). Pure D_2O creates the best experimental conditions to separate the contribution from protonated membrane and deuterated solvent to the integrated $\rho(x)$.

In the present work, the SFF model is used to analyze the structure of the polydispersed population of DMPC vesicles in $L_{\beta'}$, $P_{\beta'}$ and L_α phases. Two types of $\rho(x)$ functions are used for the evaluation of bilayer parameters. Parameters of the vesicle population ($\langle R \rangle$, σ for spherical shape or $\langle a \rangle$, ε, σ for elliptical shape) and of the bilayer (d, D, N_w) are calculated. The presented methods show what we can learn about vesicle structure from SANS experiment on other types of vesicular systems.

Materials and methods

Sample preparation

Dimyristoylphosphatidylcholine was a gift from Lipoid (Moscow, Russia). D_2O (99.9% deuteration) was purchased from Isotop (St Petersburg, Russia). Samples for measurements were prepared by conventional extrusion technique. Heavy water and DMPC were mixed in a plastic tube and the tube was sealed. DMPC concentration in the sample was 15 mM (about 1 wt%). The tube content was heated to a temperature above the main phase transition temperature and then cooled down to about −20°C. The cooling–heating cycle, accompanied by sample shaking, was repeated four times. From the dispersion of MLVs thus obtained, extruded ULVs were prepared in a single-step procedure according to MacDonald et al. (1991) using the LiposoFast Basic extruder (Avestin, Ottawa, Canada). The ULVs populations were prepared by extrusion through one polycarbonate filter (Nucleopore, Plesanton, USA) with pores of 500 Å (namely 500 Å extruded vesicles) or 1,000 Å (namely 1,000 Å extruded vesicles) diameter, mounted in the extruder fitted with two gas-tight Hamilton syringes (Hamilton, Reno, USA). The sample was subjected to 25 passes through the filter at a temperature higher than the main phase transition temperature of the DMPC. An odd number of passes was performed to avoid contamination of the sample by large and multilamellar vesicles, which might not have passed through the filter. The sample was filled into a quartz cuvette (Hellma, Müllheim, Germany) with a 2 mm sample thickness. Samples for DSC were prepared in H_2O and D_2O as dispersion of MLVs with 20% of the DMPC (w/w).

SANS measurements

The SANS spectra were collected from ULVs as function of temperature in the temperature interval 10–60°C in the range of scattering vector q from 0.02 to 0.15 $Å^{-1}$ and at $T = 30$°C in the range 0.0083 $Å^{-1} \leq q \leq 0.2$ $Å^{-1}$ from YuMO small-angle time of flight spectrometer of the Frank Laboratory of Neutron Physics, JINR, Dubna, Russia (Ostanevich 1988). Spectra were also obtained from SANS-1 spectrometer of the Swiss Spallation Neutron Source at the Paul Scherrer Institute (PSI), Switzerland. Three sample-to-detector distances 2, 6 and 20 m were used to obtain the SANS data over a wide q range from 0.0033 to 0.56 $Å^{-1}$. Neutron wavelength was 4.7 Å. $T = 10$, 20 and 30°C were chosen as temperatures of the $L_{\beta'}$, $P_{\beta'}$ and L_α phases of the DMPC in D_2O, respectively, according to our DSC results and X-ray diffraction study (Kobayashi and Fukado 1998). Netzsch DSC 200 was used for differential thermal analysis. DSC curves were recorded at the heating rate 1°C/min.

Evaluation of vesicle parameters from SANS curve

The simplest method of membrane thickness characterization is the Guinier approximation of scattering curve (Guinier and Fournet 1955; Feigin and Svergun 1987).

The macroscopic cross-section of ULVs population with $R > d$ can be presented as

$$\frac{d\Sigma}{d\Omega}(q) = n\frac{d\Sigma}{d\Omega}(0)q^{-2}\exp(-R_t^2q^2), \quad (3)$$

where n is the number of vesicles per unit volume, and

$$R_t^2 = \frac{d_G^2}{12}. \quad (4)$$

Radius of gyration R_t is determined from the Guinier plot $\left(\ln\left[\frac{d\Sigma}{d\Omega}(q)q^2\right]\text{ vs. }q^2\right)$ and membrane thickness parameter d_G is calculated from (4) (Knoll et al. 1981; Gordeliy et al. 1993). The vesicle radius and polydispersity cannot be determined in the Guinier approximation. Equation (4) is valid for the case of a large value of contrast, when the scattering length density of D_2O is larger than the average scattering length density of the bilayer. This is true for the case of "dry" bilayers, when the penetration of D_2O molecules inside the bilayer is negligibly small (Ibel and Stuhrmann 1975; Gordeliy et al. 1993). For DMPC vesicles in D_2O, the penetration of water molecules into the hydrophilic part of the bilayer influences the neutron scattering length density distribution (Kiselev et al. 2004). That is why d_G is smaller relative to the real membrane thickness d (Balgavy et al. 1998; Kiselev et al. 2001). The values of d_G and d are different on some constant Δd_H:

$$d = d_G + \Delta d_H. \quad (5)$$

A value of Δd_H depends on the penetration depth d_W of the D_2O molecules inside the bilayer and bilayer hydration (quantity of the D_2O molecules in the bilayer). A value of Δd_H is approximately equal to half the value of d_W and this simple ratio $\Delta d_H \approx d_W/2$ could be applied for the qualitative estimations.

The model of SFF was proposed for an evaluation of the vesicle radius, the polydispersity and the internal membrane structure (Kiselev et al. 2002). The coherent macroscopic cross-section of the monodispersed population of vesicles is defined by the formula:

$$\frac{d\Sigma}{d\Omega_{mon}}(q) = nA^2(q)S(q), \quad (6)$$

where n is the number of vesicles per unit volume, $A(q)$ the scattering amplitude of a vesicle and $S(q)$ the vesicle structure factor (Feigin and Svergun 1987; Kiselev et al. 2003a). For spherical ULV with radius R (Kiselev et al. 2002)

$$A(q) = 4\pi\int_{-d/2}^{d/2}\rho_c(x)\frac{\sin[(R+x)q]}{(R+x)q}(R+x)^2dx, \quad (7)$$

where $\rho_c(x) = \rho_{D2O} - \rho(x)$ is contrast, the difference between neutron scattering length densities of the bilayer $\rho(x)$ and the heavy water ρ_{D2O}. Integration of (7) gives an exact expression for the scattering amplitude of vesicle with separated parameters R, d and $\rho(x)$:

$$A_{ves}(q) = 4\pi\frac{R^2}{qR}\sin(qR)\int_{-d/2}^{d/2}\rho_c(x)\cos(qx)dx + 4\pi\frac{R}{qR}\cos(qR)\int_{-d/2}^{d/2}\rho_c(x)x\sin(qx)dx. \quad (8)$$

In the case of $R >> d/2$, $R + x \approx R$, one can neglect the second term with respect to the one in (8) (Kiselev et al. 2002). The first term in (8) presents the SFF model of the SANS scattering for vesicles. The coherent macroscopic cross-section of monodispersed population of vesicles in the frame of SFF model is written as

$$\frac{d\Sigma}{d\Omega_{mon}}(q) = nF_s(q,R)F_b(q,d)S(q), \quad (9)$$

where $F_s(q, R)$ is a form factor of the infinitely thin sphere with radius R,

$$F_s(q,R) = \left(4\pi\frac{R^2}{qR}\sin(qR)\right)^2, \quad (10)$$

and $F_b(q, d)$ is a form factor of the symmetric lipid bilayer,

$$F_b(q,d) = \left(\int_{-d/2}^{d/2}\rho_c(x)\cos(qx)dx\right)^2. \quad (11)$$

The SFF model allows the characterization of deformations of the vesicle shape from spherical to elliptical. In this case, instead of $F_s(q, R)$, the form factor of the infinitely thin ellipse $F_E(q, a)$ is written as

$$F_E(q,a) = \int_0^1 A_E^2\left(qa\sqrt{1+x^2(\varepsilon^2-1)}\right)dx, \quad (12)$$

where ε is an ellipse eccentricity, a a minor semi-axis and the function $A_E(z) = 4\pi\varepsilon a^2(\sin(z)/z)$.The polydispersity of vesicle population is described by non-symmetrical Schulz distribution (Hallet et al. 1991; Schmiedel et al. 2001):

$$G(R,\langle R\rangle) = \frac{R^m}{m!}\left(\frac{m+1}{\langle R\rangle}\right)^{m+1}\exp\left[-\frac{(m+1)R}{\langle R\rangle}\right], \quad (13)$$

where $\langle R\rangle$ is an average vesicle radius and m a coefficient of polydispersity. Relative standard deviation of the vesicle radius is given by $\sigma = \sqrt{1/(m+1)}$.

Thus, the coherent macroscopic cross-section of polydispersed vesicle population $I_{theor}(q, \langle R\rangle, d)$ is calculated as

$$I_{theor}(q,\langle R\rangle,d) = \frac{\int_{R_{min}}^{R_{max}}\frac{d\Sigma}{d\Omega_{mon}}(q,R,d)G(R,\langle R\rangle)dR}{\int_{R_{min}}^{R_{max}}G(R,\langle R\rangle)dR}, \quad (14)$$

where R_{min} and R_{max} depend on the diameter of a polycarbonate filter.

The experimentally measured macroscopic cross-section does not fully equal the theoretically calculated value of the coherent macroscopic cross-section $I_{theor}(q, \langle R\rangle, d)$ due to the incoherent scattering background IB from a sample and spectrometer resolution distortions. The experimentally measured macroscopic cross-section $d\Sigma(q)/d\Omega$ is approximated with good accuracy as

$$\frac{d\Sigma}{d\Omega}(q) = I_{theor}(q, \langle R\rangle, d) + \frac{1}{2}\Delta^2 \frac{d^2 I_{theor}(q, \langle R\rangle, d)}{dq^2} + IB, \quad (15)$$

for the case of $(\Delta/q) \leq 0.2$, where Δ^2 is a second moment of a spectrometer resolution function (Ostanevich 1988).

Equation (15) was applied to fit the SANS data using the standard minimization and error analysis program DFUMIL from the JINRLIB library (http://www.jinr.ru/programs/jinrlib). This code is the extended version of the subroutine FUMILI D510 from the CERN Program Library. Main principals of numerical algorithm are described in Dymov et al. (2000) and references therein. Details of the error analysis method on the basis of negative logarithm of likelihood function can be found in Eadie and Dryan (1971). To estimate the fit quality, we used the χ^2 functional:

$$\chi^2 = \frac{1}{N-k}\sum_{i=1}^{N}\left(\frac{\frac{d\Sigma}{d\Omega}(q_i) - \frac{d\Sigma}{d\Omega_{exp}}(q_i)}{\delta(q_i)}\right)^2, \quad (16)$$

where $\delta(q_i)$ are experimental errors of $d\Sigma_{exp}(q)/d\Omega$, N the number of experimental points and k the number of fitting parameters.

In the case of hydrophobic–hydrophilic (HH) approximation of $\rho(x)$ and with the spherical form of vesicles we have six free parameters: the number of vesicles per unit volume n, the average vesicle radius $\langle R\rangle$, the coefficient of polydispersity m, the thickness of the lipid bilayer d, the thickness of the hydrophobic bilayer part D and the value of the incoherent background IB. In the case of the elliptical form of vesicles, the elliptical vesicles eccentricity ε is added as an additional free parameter. The average vesicle radius $\langle R\rangle$ is replaced by the average value of the minor semi-axis $\langle a\rangle$. So, the number of free parameters is equal to 7.

In the case of step function (SF) approximation of $\rho(x)$ we add into the list of free parameters the average scattering length density of the polar head group ρ_{PH} and remove parameter D. In this case, the value of $D = d - d_{PH}$, where $d_{PH} = 9$ Å is a known thickness of polar head groups. So, the number of free parameters of SF approximation for the spherical form of vesicle and the elliptical form of vesicles is equal to 6 and 7, respectively.

The important question is what could be the more appropriate type of $\rho(x)$ function. This problem was analyzed by X-ray reflectometry from the lipid monolayer (Schalke et al. 2000). For the case of SANS, the $\rho(x)$ function based on the step function plus water distribution function can describe well the membrane form factor in the range $2\pi/d \leq q \leq 4\pi/d$. The membrane form factor for $q > 4\pi/d$ could be described only based on Gaussian functions. Our case is the region of $2\pi/d \leq q \leq 4\pi/d$.

Different regions of SANS curve are important for the determination of different vesicle parameters. Parameter n is a scaling factor for the congruent shift of the calculated SANS curve relative to the experimental one. It can be determined from a single experimental point. The value of IB is mainly determined from the end of the scattering curve $q > 0.3$ Å^{-1}. Parameters of the vesicle size $\langle R\rangle$ and polydispersity σ are mainly determined from the scattering curve in the region from 0.0033 Å^{-1} to about 0.03 Å^{-1} (Kiselev et al. 2003b). The important region to define parameters of $\rho(x)$ functions is $q > 0.03$ Å^{-1} (Kucerka et al. 2004c). It was shown by Kiselev et al. (2001, 2003b) that membrane thickness cannot be evaluated from SAXS curve collected in the region of 0.005 Å$^{-1} \leq q \leq 0.04$ Å^{-1} for 1% DMPC concentration. On the contrary, evaluation of the vesicle radius is not possible from the SANS curve collected in the region of 0.035 Å$^{-1} \leq q \leq 0.1$ Å^{-1} (Kucerka et al. 2004b) or 0.021 Å$^{-1} \leq q \leq 0.36$ Å^{-1} (Schmiedel et al. 2005).

Results and discussion

Dependence of the membrane thickness on temperature, Guinier approximation

It was shown recently via DSC that D_2O influences the phase transition properties of three phospholipid membranes: DPPC, DSPC, DHPC (Matsuki et al. 2005). The DSC thermal analysis was carried out to clarify the influence of D_2O on the phase transitions of DMPC. Figure 1 presents the DSC curves recorded on MLVs of DMPC in H_2O and D_2O. By solvent substitution of H_2O by D_2O, a noticeable shift of the pre-transition and main phase transition peaks is observed. The temperatures and enthalpies (ΔH) of phase transitions were determined from the DSC thermograms and the results are listed in Table 1. The raise in the main transition temperatures of DMPC in D_2O is about 0.6°C. Unlike the main transition temperature, the variation of pre-transition temperature was +1.6°C as compared to H_2O. The ΔH values showed the same trends as the transition temperatures; they increased in all the transitions.

Figure 2 presents the dependence of DMPC membrane thickness parameter d_G on temperature. DMPC vesicles were prepared by extrusion through pores with diameter 1,000 Å. SANS spectra were collected using YuMO spectrometer. Values of d_G were evaluated in the Guinier plot via (3) and (4). The membrane thickness parameter d_G is found to be 44.2 ± 0.8 Å at $T = 10$°C ($L_{\beta'}$ phase), 43.4 ± 0.8 Å at $T = 20$°C ($P_{\beta'}$ phase) and

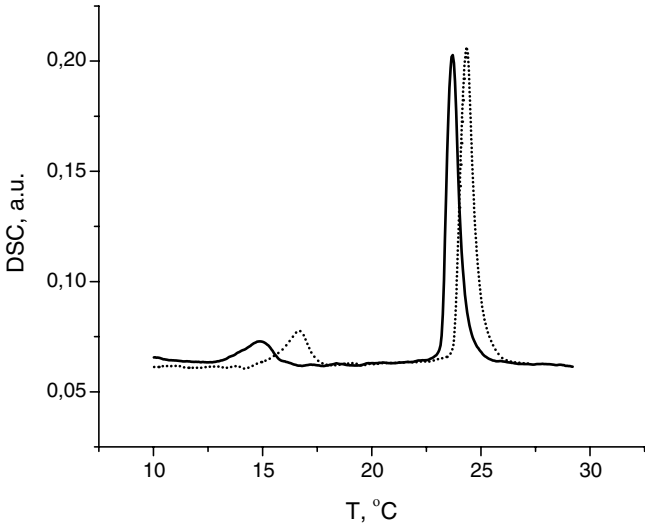

Fig. 1 Differential scanning calorimetry curves from MLVs of DMPC in H_2O (*solid line*) and D_2O (*dotted line*). The first endothermic peak (pre-transition) corresponds to the transition from the $L_{\beta'}$ to the $P_{\beta'}$ phase. The second endothermic peak (main phase transition) corresponds to the transition from the $P_{\beta'}$ to the L_α phase

Table 1 D_2O's influence on the DMPC phase transition properties

Solvent	T_p (°C)	ΔH_p (cal/g)	T_m (°C)	ΔH_m (cal/g)
H_2O	14.9	1.3	23.2	8.1
D_2O	16.7	1.6	23.8	8.6

T_p (peak position) and ΔH_p are pre-transition temperature and enthalpy, T_m (onset) and ΔH_m are main phase transition temperature and enthalpy, respectively

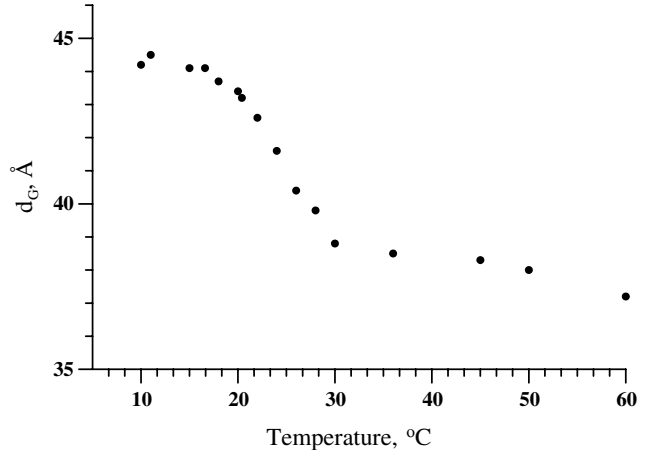

Fig. 2 Dependence of DMPC membrane thickness parameter d_G on temperature for the 1,000 Å extruded vesicles. Values of d_G were evaluated from SANS curves in the Guinier approximation

38.8 ± 0.8 Å at $T = 30$°C (L_α phase). These values of d_G underestimate the membrane thickness d relative to the data from the X-ray diffraction experiment which are 48.2 Å at $T = 10$°C and 44.2 Å at $T = 30$°C (Nagle and Tristram-Nagle 2000; Tristram-Nagle et al. 2002). The value of Δd_H in (5) is equal to 4 Å in the $L_{\beta'}$ and 5.4 Å in the L_α phase of DMPC, which reflects increased DMPC hydration in the L_α phase. The Guinier approximation describes the relative changes in the membrane thickness under temperature alteration rather well. Figure 2 demonstrates the decrease in the membrane thickness at the main phase transition temperature of 23.8°C. The membrane thickness decreases on the value of 5.4 ± 1.6 Å on heating from 10 to 30°C in concurrence with a 4 Å decrease obtained from X-ray diffraction experiment.

What is the appropriate ρ(x) approximation and fitting procedure?

The important question is the choice of the appropriate $\rho(x)$ approximation and the number of free fitting parameters. In this section we present our fitting results, obtained for three approximations of $\rho(x)$ known from the literature (Kucerka et al. 2004c). These approximations are presented in Fig. 3a–c. The fixed parameters of these approximations are the neutron scattering length density of D_2O, $\rho_{D2O} = 6.33 \times 10^{10}\,\mathrm{cm}^{-2}$, and the neutron scattering length density of hydrocarbon chains, $\rho_{CH} = -0.36 \times 10^{10}\,\mathrm{cm}^{-2}$ (Schmiedel et al. 2001). The most simple case is the homogeneous approximation of the neutron scattering length density of the lipid bilayer, $\rho(x) = \mathrm{const}$, namely approximation (a). Approximation (a) has two free parameters, the membrane thickness d and the average neutron scattering length density of the lipid bilayer ρ_{av}. More realistic is the approximation of the membrane structure as the region of the hydrocarbon chains with thickness D and the region of the polar head groups with thickness $(d-D)/2$, approximation (b). Free parameters of step function approximation (b) are the membrane thickness d, the thickness of the hydrocarbon chain region D and the average neutron scattering length density of the polar head group region ρ_{PH}. Approximation (c) has the same number of free parameters, but more complex scattering length density distribution in the region of polar head groups. Linear D_2O distribution inside the polar head group region was introduced in the approximation (c) in addition to the step function type of $\rho(x)$ from dry bilayer. These three approximations of the $\rho(x)$ were used to fit the experimental SANS spectrum at $T = 30$°C for 500 Å extruded vesicles. The results are presented in Table 2. Obtained values of the average radius and the polydispersity for approximations (b) and (c) are in good agreement and are little bit different from the approximation (a). This difference of about 2 Å in the values of the radius of infinitely thin spheres can be used as an accuracy of the average radius determination for vesicles.

For the case of homogeneous approximation (a) it is convenient to use in the equations the average contrast $\Delta\rho = \rho_{D2O} - \rho_{av}$ instead of ρ_{av}. On the contrary, the value of ρ_{av} is more suitable for presentation in figures

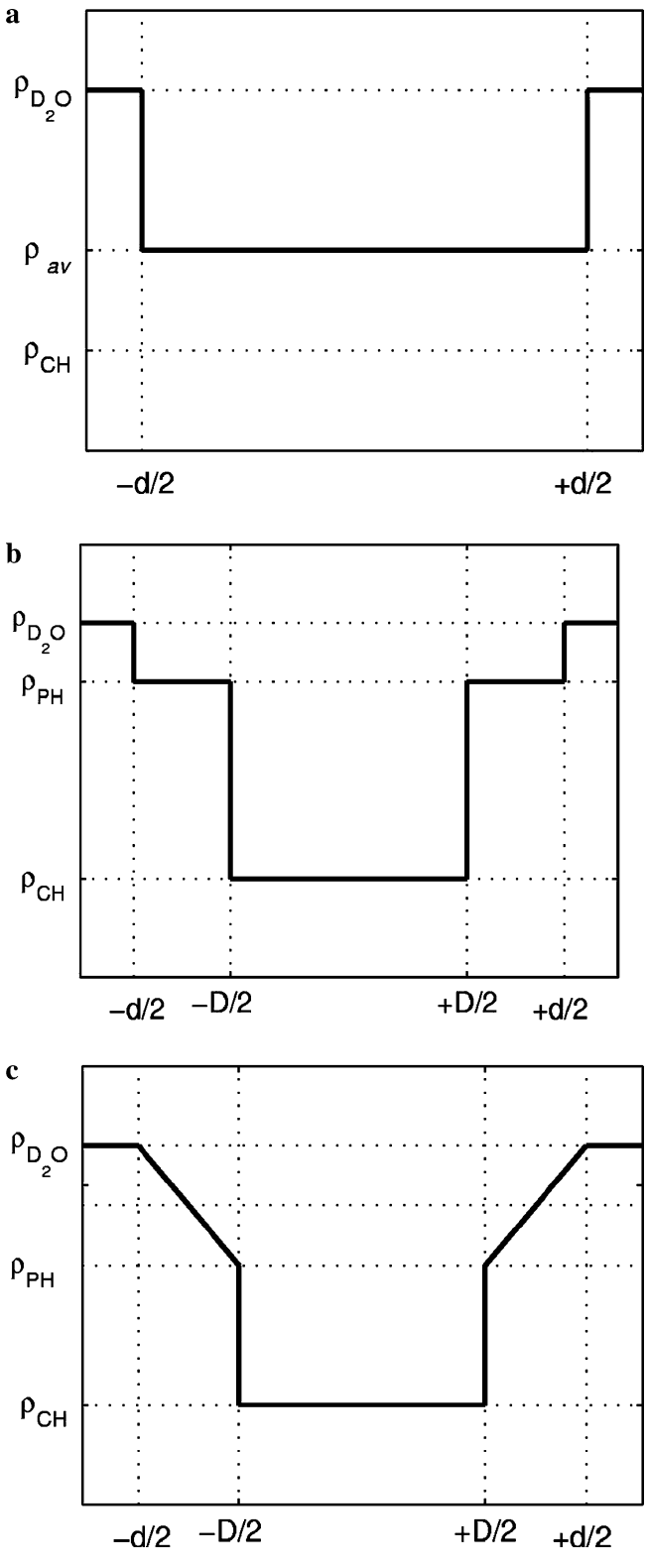

Fig. 3 **a** Homogeneous approximation of the neutron scattering length density across the lipid bilayer, $\rho(x) = \rho_{av} = \text{const}$ or $\rho_c(x) \equiv \Delta\rho = \text{const}$. d is the membrane thickness and ρ_{av} the average scattering length density of the bilayer. Approximation (a). **b** Step function (SF) approximation of the neutron scattering length density across the lipid bilayer $\rho(x)$ with free parameters of the polar head group. d is the membrane thickness, D the thickness of the hydrocarbon chain region and ρ_{PH} the scattering length density in the region of the polar head group. Approximation (b). **c** Step function (SF) approximation of the neutron scattering length density across the lipid bilayer $\rho(x)$ with linear water distribution inside the polar head group. d is the membrane thickness, D the thickness of the hydrocarbon chain region and ρ_{PH} the scattering length density of the polar head group. Approximation (c)

and tables. In this case, (11) is integrated to the following form (Kiselev et al. 2002):

$$F_{b,hom}(q,d) = \left(\frac{2\Delta\rho}{q}\sin\left(\frac{qd}{2}\right)\right)^2, \quad (17)$$

and we obtain the factor $n(\Delta\rho)^2$ in (9). The value of n has to be known for the determination of $\Delta\rho$ and therefore ρ_{av} from the fitting procedure. The number of vesicles per cm^3 $n(R, d)$ depends on the vesicle radius and the membrane thickness. The value of $n(R, d)$ is calculated from the DMPC concentration in the sample as

$$n(R,d) = \frac{C}{N_{DMPC}(R,d)}, \quad (18)$$

where C is the number of DMPC molecules per cm^3 and $N_{DMPC}(R, d)$ the number of DMPC molecules in the single vesicle with radius R and membrane thickness d. The concentration of DMPC in our experiment is 15 mM. The number of DMPC molecules per cm^3 is calculated to be $C = 15 \times 10^{-3} \times N_A \times 10^{-3} = 90.4 \times 10^{17}$, where N_A is the Avogadro's number. It is known that the molecular volume of DMPC in the liquid L_α phase is equal to 1,101 Å^3 (Nagle and Tristram-Nagle 2000). The volume of the lipid bilayer of a single vesicle can be calculated by the formula $V = 4\pi/3\,[(R + d/2)^3 - (R - d/2)^3]$. So, $N_{DMPC}(R, d) = V/1{,}101$ is the number of DMPC molecules in a single vesicle. Similar to the approximation (a), (18) was used in the approximations (b) and (c) for calculations of $n(R, d)$.

Results of the experimental spectrum fitting are presented in Table 2. The obtained value of the average contrast $\Delta\rho = 4.84 \times 10^{10}$ cm^{-2} corresponds to the $\rho_{av} = 1.49 \times 10^{10}$ cm^{-2}. The scattering length of the DMPC molecule is 3.1×10^{-12} cm^{-2}, the volume of the dry DMPC molecule is 1,101 Å^3. Thus, the average scattering length density of the dry DMPC molecule is equal to 0.28×10^{10} cm^{-2}. The value of the membrane thickness $d = 36.7$ Å obtained in the homogeneous approximation is smaller than $d = 44.2$ Å from X-ray diffraction experiment (Nagle and Tristram-Nagle 2000). These differences in ρ_{av} and d can be explained by the effect of penetration of D_2O molecules in the lipid bilayer (Kiselev et al. 2004). D_2O penetration increases the value of ρ_{av} and makes the part of the bilayer near the membrane surface invisible for neutrons. Thus, homogeneous approximation is not appropriate for the evaluation of membrane thickness. This conclusion is supported by the large value of $\chi^2 = 18.7$ and the differences in the experimental and fitted spectra as presented in Fig. 4a. The fitted curve is in good agreement

Table 2 Parameters of 500 Å extruded DMPC vesicles in the L_α phase ($T = 30°C$) calculated in the framework of SFF model for three different approximations of the $\rho(x)$ presented in Fig. 3a–c

Approximation	⟨R⟩(Å)	σ (%)	d (Å)	D (Å)	ρ (10^{10} cm^{-2})	IB (10^{-3} cm^{-1})	χ^2
(a)	272.9 ± 0.4	28	36.7 ± 0.02		$\rho_{av} = 1.49 \pm 0.005$	5.01 ± 0.01	18.7
(b)	275.3 ± 0.4	27	46.4 ± 0.03	18.10 ± 0.03	$\rho_{PH} = 3.40 \pm 0.003$	5.76 ± 0.01	4.05
(c)	275.0 ± 0.4	27	47.4 ± 0.04	17.30 ± 0.05	$\rho_{PH} = 4.90 \pm 0.001$	5.90 ± 0.01	3.62

⟨R⟩ is the average vesicle radius, σ the vesicle polydispersity, d the membrane thickness, D the thickness of the hydrocarbon chains. Sense of the ρ parameters is presented in Fig. 3a–c. IB is the value of incoherent background, χ^2 is a fit quality parameter. Accuracy of σ is about 1%

with the experimental curve up to $q = 0.17$ Å^{-1}. This value of q determines the homogeneous region of SANS curve. The homogeneous region of SANS curve is larger than the region of Guinier approximation which is limited by $q = 0.14$ Å^{-1}.

Application of SF approximation (b) with free parameters d, D and ρ_{PH} gives good agreement between experimental and fitted curves as seen in Table 2 ($\chi^2 = 4.05$) and Fig. 4b. The obtained value of $d = 46.4$ Å

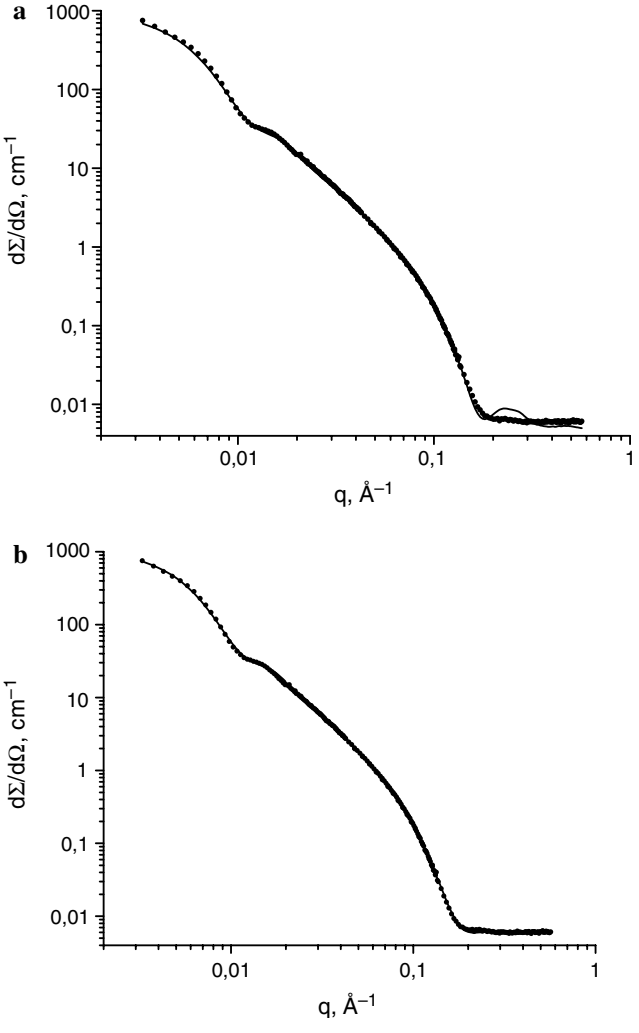

Fig. 4 Experimental macroscopic cross-section of the ULVs population at $T = 30°C$ (*dots*) for vesicles extruded through pores of 500 Å diameter and fitting curve (*solid line*). **a** Homogeneous approximation $\rho(x) = \text{const}$ presented in Fig. 3a. **b** Approximation (b) of $\rho(x)$ presented in Fig. 3b

is reasonable, but the value of D is too small. The obtained thickness of the polar head group region $d_{PH} = (d - D)/2 = 14.2$ Å is unreasonably larger than the value of 9 Å from X-ray diffraction (Nagle and Tristram-Nagle 2000) and the value of 8 Å from SANS based on the Gaussian approximation of $\rho(x)$ in the region of polar head groups (Kiselev et al. 2004). Similar to the approximation (b) an application of the approximation (c) requires three fitting parameters for the description of the internal bilayer structure (d, D and ρ_{PH}). Linear water distribution inside the polar head group region improves the agreement between experimental and fitted curves ($\chi^2 = 3.62$) and increases the value of membrane thickness to 47.4 Å, but similar to SF approximation (b) gives unreasonably large thickness of the polar head region 15.1 Å. The results obtained in the approximations (b) and (c) show that the fitting procedure decreases the value of D to the value of hydrophobic–hydrophilic boundary. The water distribution function across the bilayer has sigmoidal form (Armen et al. 1998; Kiselev et al. 2004). In the L_α phase, the contribution from D_2O distribution function to the integrated neutron scattering length density of DMPC is sufficiently larger than the one from the polar head group (Kiselev et al. 2004). This is the reason why our approximations based on two free parameters of polar head group (D, ρ_{PH}) cannot describe the internal structure of the bilayer correctly. The second disadvantage of the used approach is the relationship between R and d via (18) in the calculation of $n(R, d)$. This connection is in conflict with the ideology of SFF model, which is to separate R and d. Moreover, calculations of $n(R, d)$ complicate the convergence process due to the system polydispersity. The described approximations give reasonable values of the average radius and the membrane thickness, but are not appropriate for the determination of the internal membrane structure. More appropriate approximations of $\rho(x)$ are the subject of the next paragraphs.

Note that the accuracy of calculated parameters depends on the statistical errors in the measured scattering intensity and the interval of q used. Statistical errors of SANS PSI spectra are smaller than 2%. This is the reason why parameter errors in Table 2 are so small. For comparison, the same calculations have been performed with the SANS spectra measured using YuMO small-angle spectrometer in the q range from 0.0083 to 0.2 Å^{-1} with statistical errors growing from 2% at the small q to 30–50% at $q \approx 0.2$ Å^{-1}, see Fig. 7. In this

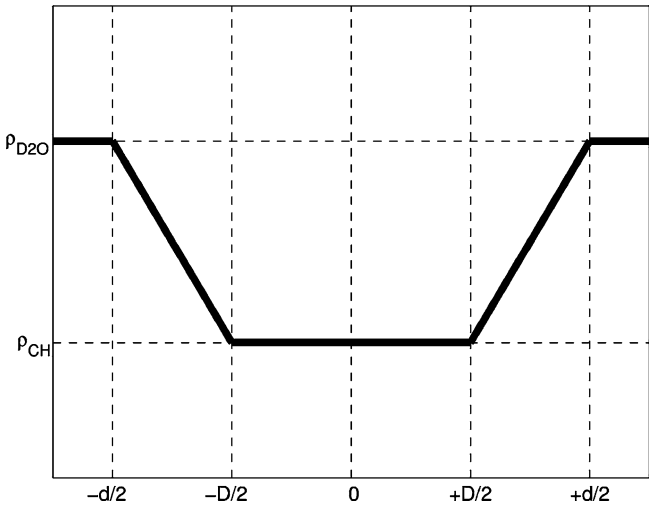

Fig. 5 Hydrophobic–hydrophilic (HH) approximation of the neutron scattering length density across the lipid bilayer $\rho(x)$. d is the membrane thickness and D the thickness of the hydrophobic part of the membrane

case, the parameter errors are significantly larger: homogeneous approximation (a): $\langle R\rangle = 277 \pm 5$ Å, $\sigma = 30 \pm 1\%$, $d = 36.7 \pm 0.1$ Å, $\rho_{av} = (1.30 \pm 0.01) \times 10^{10}\text{cm}^{-2}$, $\chi^2 = 1.31$; SF approximation (b): $\langle R\rangle = 277 \pm 5$ Å, $\sigma = 30 \pm 1\%$, $d = 42.1 \pm 0.4$ Å, $D = 13.2 \pm 0.7$ Å, $\rho_{PH} = (4.1 \pm 0.1) \times 10^{10}\text{cm}^{-2}$, $\chi^2 = 1.15$.

DMPC vesicles in the L_α phase, the HH approximation of $\rho(x)$

The hydrophobic–hydrophilic approximation of the internal bilayer structure is used as $\rho(x)$ function in the L_α phase of DMPC. It is based on the fact that the neutron scattering length density of D_2O molecules in the hydrophilic region of the bilayer is sufficiently larger than the neutron scattering length density of polar head groups in the L_α phase of DMPC (Kiselev et al. 2004). The HH approximation of $\rho(x)$ is presented in Fig. 5 (Schmiedel et al. 2005). The lipid bilayer consists of two parts: hydrophobic and hydrophilic. Linear approximation is used for the water distribution function in the hydrophilic region, where $\rho_{D2O} = 6.33 \times 10^{10}$ cm^{-2} and $\rho_{CH} = -0.36 \times 10^{10}$ cm^{-2} are fixed parameters of neutron scattering length densities. The parameters of the DMPC bilayer determined from the SANS curve are the membrane thickness d and the thickness of the hydrophobic part D.

The number of water molecules N_w and the surface area per DMPC molecule A are determined from the system:

$$A\frac{d}{2} = V_{DMPC} + N_w V_{D2O}, \tag{19}$$

$$A\left(\rho_{CH}\frac{D}{2} + \frac{\rho_{D2O} - \rho_{CH}}{2}\frac{d-D}{2}\right) = l_{DMPC} + N_w, \tag{20}$$

where $V_{DMPC} = 1{,}101$ Å^3 and $V_{D2O} = 30$ Å^3 are molecular volumes of DMPC and D_2O, $l_{DMPC} = 3.07 \times 10^{-12}$ cm and $l_{D2O} = 1.92 \times 10^{-12}$ cm are neutron scattering lengths of DMPC and D_2O molecules, respectively. Let us denote $l' = l_{DMPC}/l_{D2O}$ and $V' = V_{DMPC}/V_{D2O}$. One can define the average neutron scattering length density of hydrated DMPC as

$$\bar{\rho} = \frac{D}{d}\rho_{CH} + \frac{d-D}{d}\frac{\rho_{D2O} - \rho_{CH}}{2}. \tag{21}$$

The solution of (19) and (20) is

$$N_w = \frac{\bar{\rho}V' - \rho_{D2O}l'}{\rho_{D2O} - \bar{\rho}}, \quad A = 2 \times \frac{V_{DMPC} + N_w V_{D2O}}{d}. \tag{22}$$

Extruded 500 Å vesicles

Figure 6 shows the experimentally measured and fitted SANS curves for the DMPC ULVs at $T = 30$°C. ULVs were prepared by extrusion through pores with the diameter 500 Å. The experimentally measured macroscopic cross-section was calculated by two different methods: by application of the exact expression for the scattering amplitude using (8) and by application of the SFF model using (9). This allows one to check a validity of the SFF model and estimate a contribution of the second term in (8). The obtained parameters are given in Table 3. Parameters of vesicle populations and internal membrane structure evaluated by exact expression and by SFF model for scattering amplitude coincide exactly. The second term in (8) improves χ^2 without any influence on the accuracy of the evaluated parameters.

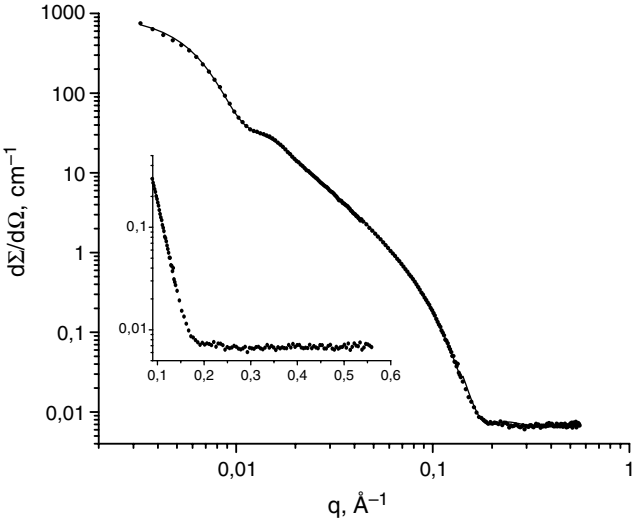

Fig. 6 Experimental macroscopic cross-section of the ULVs population at $T = 30$°C (*dots*) for vesicles extruded through pores of 500 Å diameter and fitting curve (*solid line*). HH approximation of $\rho(x)$ presented in Fig. 5. The *inset* shows the magnified curve for large q

The obtained value of $\langle R\rangle = 275.6 \pm 0.5$ Å is in concurrence with the radius of the pores (250 Å) used during vesicle extrusion. The membrane thickness d, evaluated on the basis of the HH approximation of $\rho(x)$, is equal to 47.8 ± 0.2 Å, whereas the thickness of the hydrophobic region D is 20.5 ± 0.3 Å and of the membrane hydrophilic part, $D_H = (d - D)/2 = 13.7 \pm 0.5$ Å. The latter is larger than that of the polar head groups $D_{PH} = 9$ Å, evaluated from X-ray diffraction (Nagle and Tristram-Nagle 2000), or $D_{PH} = 8.1 \pm 1.7$ Å, evaluated from SANS (Kiselev et al. 2004). This result shows that water molecules penetrate into the hydrocarbon chain region at 4.7 Å. The value of membrane thickness $d = 47.8 \pm 0.2$ Å is 3.6 Å larger than $d = 44.2$ Å evaluated from X-ray diffraction experiment on the giant MLVs (Nagle and Tristram-Nagle 2000). The number of water molecules $N_w = 11.9 \pm 0.3$ and surface area $A = 61.0 \pm 0.4$ Å^2 of the DMPC molecule differ from $N_w = 7.2$ and $A = 59.6$ Å^2 for the giant MLVs (Nagle and Tristram-Nagle 2000). Hydration and membrane thickness of the curved DMPC bilayer are larger relative to the flat bilayer. Similar results were obtained recently for POPC membrane structure as function of vesicle radius (Schmiedel et al. 2005).

The form of vesicles in the liquid L_α phase cannot be ideally spherical. Probably, the vesicle shape fluctuates near the spherical form. These fluctuations serve as the origin of the ULVs deformation and orientation in the strong magnetic field. ULVs deformation in the strong magnetic field of 4 T has been detected via SANS (Kiselev et al., unpublished). The elliptical form of the vesicle shape can be taken into account on the basis of (12). Table 3 presents the results for the case of 500 Å extruded vesicles, assuming that their form is elliptical. The value of eccentricity is 1.1, which demonstrates that the vesicle shape is close to a sphere. Nevertheless, the membrane thickness has a value of 48.9 ± 0.2 Å at $\varepsilon = 1.1$ in comparison with $d = 47.8 \pm 0.2$ Å for $\varepsilon = 1$. The difference between these two values of d is 1.1 Å. Parameters of the bilayer, d and D, are evaluated from the membrane form factor $F_b(q, d)$, which does not depend on the value of ε in the SFF model. In the same approximation of $\rho(x)$ no reason exists for the difference in the value of d. So, the value of 1.1 Å characterizes the accuracy of the membrane thickness evaluation from the SANS curve collected in q range from 0.0033 to 0.56 Å^{-1}. Decreasing the q range to the interval 0.0083 Å$^{-1} \le q \le 0.2$ Å^{-1} and increasing the statistical errors, as shown in Fig. 7 for 500 Å extruded vesicles, decrease the accuracy of the parameter evaluation. The parameters of vesicle population in the L_α phase evaluated via HH approximation from SANS spectra measured using YuMO spectrometer (see Fig. 7) are: $\langle R\rangle = 277 \pm 5$ Å, $\sigma = 31 \pm 1\%$, $d = 48.9 \pm 0.7$ Å, $D = 20 \pm 3$ Å, $N_w = 12 \pm 3$, $A = 60 \pm 3$ Å^2, $\chi^2 = 1.08$. It is shown in Table 2 that χ^2 for the $\rho(x)$ approximations (a), (b) and (c) are worse than χ^2 for HH approximation presented in Table 3. Similar results were obtained in the case of spectrum measured using YuMO spectrometer: $\chi^2 = 1.31$ for the approximation (a), $\chi^2 = 1.15$ for the approximations (b) and (c) and $\chi^2 = 1.08$ for the HH approximation. The results from two different instruments taken together show that the HH approximation is more appropriate for the modeling of DMPC bilayer structure in the L_α phase.

Extruded 1,000 Å vesicles

Figure 8 demonstrates the experimental macroscopic cross-section of the ULVs population at $T = 30$°C and fitting curve for 1,000 Å extruded vesicles. The results of the fit are presented in the Table 3. Figure 9 demonstrates the comparison of the experimental SANS curves recorded at 30°C for 500 and 1,000 Å extruded vesicles. The position of the first minimum in the form factor of infinitely thin sphere depends on the vesicle radius as $q_R = \pi/R$, see (10), and corresponds to the $q_{500} = 0.0126$ Å^{-1} for 500 Å extruded vesicles and $q_{1,000} = 0.0063$ Å^{-1} for 1,000 Å extruded vesicles. Vesicles prepared via extrusion through pores of 500 and 1,000 Å differ in membrane curvature and polydispersity. The polydispersity (relative standard deviation of radius) increases from 27 to 47% on increasing the vesicle radius as seen from Fig. 9.

The fitted curve cannot describe the experimental curve well in the region of sphere form factor (0.0033 Å$^{-1} \le q \le 0.03$ Å^{-1}) as shown in the inset of Fig. 8. This discrepancy between experimental and fitted curves increases the value of χ^2 in Tables 3 and 4 for

Table 3 Results for DMPC vesicles in the L_α phase ($T = 30$°C) based on the HH approximation of the $\rho(x)$

Model; D_F (Å)	$\langle R\rangle$ or $\langle a\rangle$ (Å)	ε	σ (%)	d (Å)	D (Å)	N_w	A (Å^2)	IB (cm^{-1})	χ^2
Exact; 500	275.7 ± 0.4	1	27	47.8 ± 0.2	20.5 ± 0.3	11.9 ± 0.3	61.0 ± 0.4	0.007	1.65
SFF; 500	275.6 ± 0.5	1	27	47.8 ± 0.2	20.5 ± 0.3	11.9 ± 0.3	61.0 ± 0.4	0.007	1.68
SFF; 500	266 ± 2	1.11 ± 0.02	26	48.9 ± 0.2	19.9 ± 0.4	12.8 ± 0.3	60.7 ± 0.5	0.007	1.65
SFF; 1,000	450[a]	1	48	45.5 ± 0.6	20.8 ± 0.4	10.8 ± 0.4	62.6 ± 1.0	0.007	15.50

D_F is the diameter of the pores used at extrusion, $\langle a\rangle$ the average value of the minor semi-axis, ε the eccentricity, $\langle R\rangle$ the average vesicle radius for $\varepsilon \equiv 1$, σ the vesicle polydispersity, d the membrane thickness, D the thickness of the hydrophobic core, N_w and A the number of water molecules and the surface area per DMPC molecule, respectively, IB the value of the incoherent background, χ^2 the fit quality parameter. Accuracy of σ is about 1%

[a] $\langle R\rangle = 450$ Å, $\varepsilon = 0$ from DLS (Hallet et al. 1991)

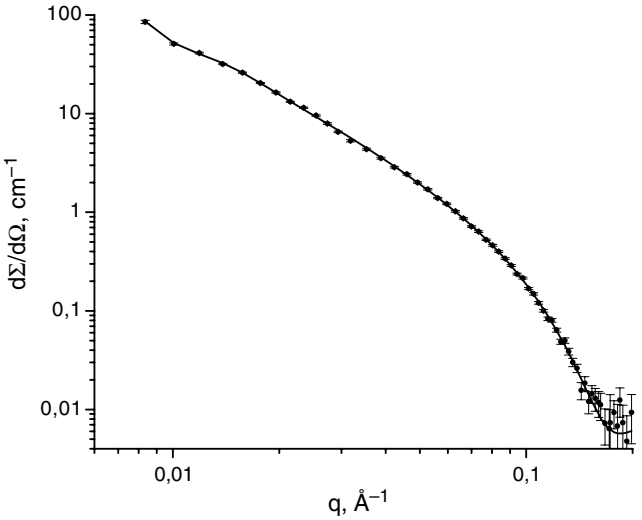

Fig. 7 Experimental macroscopic cross-section of the ULVs population at $T = 30°C$ (*dots*) for vesicles extruded through pores of 500 Å diameter and fitting curve (*solid line*). HH approximation of $\rho(x)$ presented in Fig. 5. YuMO spectrometer

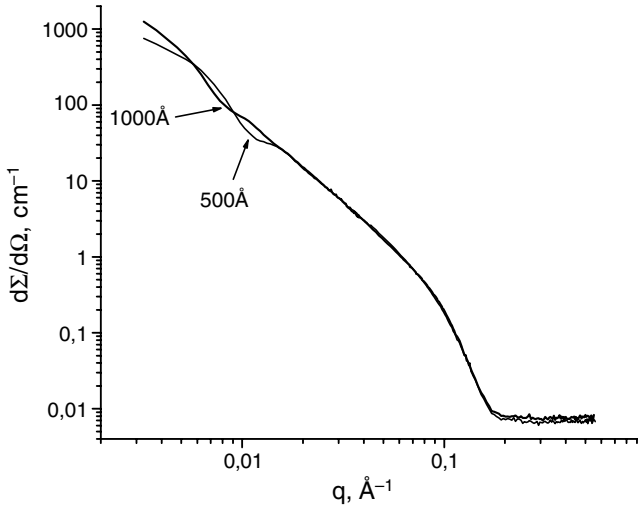

Fig. 9 Experimental macroscopic cross-sections of the ULVs populations at $T = 30°C$ for vesicles prepared by extrusion through pores of 500 and 1,000 Å diameters

1,000 Å extruded vesicles. For 1,000 Å extruded vesicles in L_α phase $\chi^2 = 15.5$ for the full q range from 0.0033 to 0.56 Å^{-1}. Calculation of χ^2 in the q range from 0.03 to 0.56 Å^{-1}, which is important for the membrane structure, demonstrates sufficiently better agreement between experimental and fitted curves, $\chi^2 = 8.7$. As a result of the discrepancy between the experiment and the fit at 0.0033 Å$^{-1} \leq q \leq 0.03$ Å^{-1}, the evaluated value of the average vesicle radius $\langle R \rangle = 314.6 \pm 0.7$ Å is sufficiently smaller than the radius of the polycarbonate pores of 500 Å. Value of $\langle R \rangle = 314.6$ Å is in contradiction to the values obtained from other methods. DLS and freeze-fracture electron microscopy results show

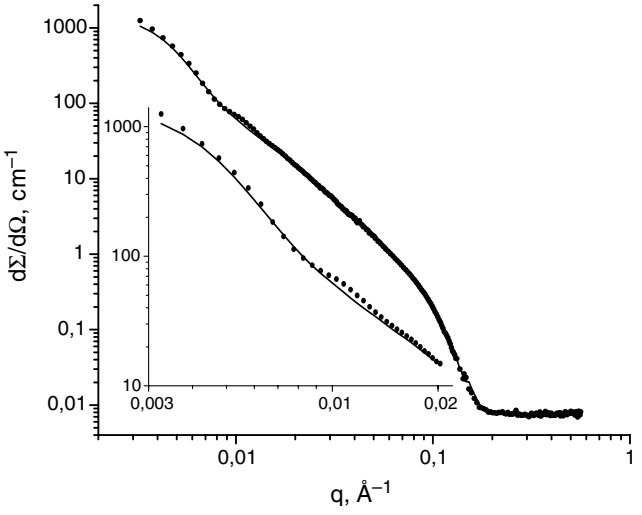

Fig. 8 Experimental macroscopic cross-section of the ULVs population at $T = 30°C$ (*dots*) for vesicles extruded through pores of 1,000 Å diameter and fitting curve (*solid line*). HH approximation of $\rho(x)$ presented in Fig. 5. The *inset* shows the magnified curve for small q

that the average vesicle radius after extrusion is about the radius of the pores (MacDonald et al. 1991; Hallet et al. 1991; Patty and Frisken 2003). The underestimation of the vesicle radius for 1,000 Å extruded vesicles has different reasons. The first reason is a big value of the vesicles polydispersity, 48%. The second is an accuracy of the correction for spectrometer resolution: $\Delta/q = 0.53, 0.27$ and 0.14 for $q = 0.0033$, 0.0063 and 0.0126 Å^{-1}, respectively (Pedersen et al. 1990). Third is the small number of experimental points: value of $q_{1,000} = 0.0063$ Å^{-1} is not so far from the value of $q_{\min} = 0.0033$ Å^{-1} (only five experimental points). Additional possible reason could be the difference between the distribution statistics of 500 and 1,000 Å extruded vesicles (Korgel et al. 1998). The careful study of vesicle form and distribution requires more powerful SANS instrument and (or) complementary application of static and dynamic light scattering. We consider $\langle R \rangle = 314.6 \pm 0.7$ Å for 1,000 Å extruded vesicle as artifact. The value $\langle R \rangle = 450$ Å from DLS is used for the characterization of 1,000 Å extruded vesicles in Tables 3 and 4 (Hallet et al. 1991).

The membrane thickness $d = 45.5 \pm 0.6$ Å is found for the ULVs prepared by extrusion through pores with diameter 1,000 Å. This value of membrane thickness is in better agreement with the value $d = 44.2$ Å as obtained for giant MLVs in H_2O. Decreasing bilayer thickness on reduction of the membrane curvature reduces the number of water molecules N_w from 11.9 ± 0.3 to 10.8 ± 0.3 and increases the surface area A from 61.0 ± 0.4 to 62.6 ± 1.0 Å^2, whereas the hydrophobic thickness D stays unchanged under the membrane curvature alteration. Our findings about the differences in the bilayer structure of the extruded ULVs and MLVs with zero curvature is supported by the experimental results presented recently in Schmiedel et al. (2005). It was shown by the systematic study of POPC vesicles

Table 4 Results for DMPC vesicles based on the SF approximation of $\rho(x)$ in the frame of SFF model

D_F (Å)	T (°C), phase	$\langle R\rangle$ or $\langle a\rangle$ (Å)	ε	σ (%)	d (Å)	ρ_{PH} (10^{10} cm^{-2})	$N_{w,PH}$	A (Å^2)	IB (cm^{-1})	χ^2
500	30, L_α	275.1 ± 0.5	1	27	45.5 ± 0.7	3.7 ± 0.2	6.8 ± 0.6	57 ± 1	0.007	2.8
1,000	30, L_α	450[a]	1	48	45.7 ± 0.7	4.0 ± 0.2	8.0 ± 0.6	59 ± 1	0.007	11.5
500	20, $P_{\beta'}$	187 ± 1	1.63 ± 0.02	22	47.9 ± 0.7	3.6 ± 0.3	5.3 ± 0.5	50 ± 1	0.006	4.5
1,000	20, $P_{\beta'}$	450[a]	1	35	48.3 ± 0.6	3.8 ± 0.2	5.9 ± 0.4	50.4 ± 0.8	0.006	19.9
500	10, $L_{\beta'}$	185 ± 1	1.62 ± 0.02	21	49.1 ± 0.7	3.7 ± 0.2	5.2 ± 0.5	48.8 ± 0.9	0.005	6.0
1,000	10, $L_{\beta'}$	450[a]	1	37	49.6 ± 0.5	3.6 ± 0.2	5.9 ± 0.5	49.2 ± 0.9	0.006	22.2

T is the temperature, D_F the diameter of the pores used at extrusion, $\langle a\rangle$ the average value of minor semi-axis, ε the eccentricity, $\langle R\rangle$ the average vesicle radius for $\varepsilon \equiv 1$, σ the vesicle polydispersity, d the membrane thickness, ρ_{PH} the scattering length density of polar head group, $N_{w,PH}$ and A the number of water molecules in the region of polar head group and surface area per DMPC molecule, respectively, IB the value of the incoherent background, χ^2 the fit quality parameter. Accuracy of σ is about 1%

[a] $\langle R\rangle = 450$ Å, $\varepsilon = 0$ from DLS (Hallet et al. 1991)

extruded through pores of 500, 1,000, 2,000 and 4,000 Å diameter that POPC membrane thickness is equal to 47, 44, 43.8 and 42.1 Å, respectively, for the different membrane curvatures. The value of A increases from 71 Å^2 for 500 Å extruded POPC vesicles to 75 Å^2 for 4,000 Å extruded POPC vesicles. The POPC bilayer hydration is also influenced by the membrane curvature. The value of N_w decreases from 13.5 for 500 Å extruded vesicles to 10.4 for 4,000 Å extruded vesicles.

Presented results are similar to those of Schmiedel et al. (2005) in that the structure and hydration of vesicle bilayer after extrusion depend on the membrane curvature in the L_α phase. The bilayer thickness and hydration are altered with increasing vesicle radius to its values for the flat bilayer. It is known that ULVs prepared via extrusion of MLVs through pores of 500–1,000 Å diameter are not time-stable system (Kiselev et al. 2003b). Probably, the membrane thickness and the hydration undergo alteration during system equilibration from the non-stable ULVs to the static state of the MLVs. One can assume that hydration of the DMPC bilayer could be the driving force in the transformation of the ULVs to the MLVs.

DMPC vesicles in the L_α phase, the SF approximation of $\rho(x)$

The SF approximation of scattering length density across the lipid bilayer $\rho(x)$ is shown in Fig. 10. The thickness of the polar head group $d_{PH} = 9$ Å was fixed as in the calculations done earlier (Kucerka et al. 2004b). Vesicle shape is considered as spherical. The difference relative to calculations in Kucerka et al. (2004b) is expressed in free value of the scattering length density in the region of polar head group ρ_{PH}. The fitting parameters of the lipid bilayer are d and ρ_{PH}. This allows one to calculate the number of water molecules located in the polar head group region $N_{w,PH}$ and the surface area A, taking into account that for SF approximation the average neutron scattering length density of hydrated DMPC is defined as

$$\bar{\rho} = \frac{d - 2D_{PH}}{d}\rho_{CH} + \frac{2D_{PH}}{d}\rho_{PH}. \quad (23)$$

The calculated parameters are given in Table 4. Inside the SF approximation, the membrane thickness $d = 45.5 \pm 0.7$ Å does not show dependence on the membrane curvature and is the same as membrane thickness for 1,000 Å extruded vesicles. Both the obtained values of the membrane thickness are larger than those of the giant MLVs (44.2 Å) in H_2O. Other fitted and calculated parameters for 500 and 1,000 Å extruded ULVs are the same within the experimental errors. Two calculated values of $N_{w,PH} = 6.8 \pm 0.6$ and $N_{w,PH} = 8.0 \pm 0.6$ are in good agreement with the data for giant MLVs 7.2 (Nagle and Tristram-Nagle 2000). Finally, the average value $N_{w,PH} = 7.4 \pm 0.6$ can characterize the number of D_2O molecules in the polar head group of DMPC at 30°C. Comparison of the hydration calculated by HH and SF approximations allows one to calculate the number of D_2O molecules in the region of hydrocarbon chains as 4.5 ± 0.9 for 500 Å and 3.4 ± 0.9 for 1,000 Å extruded vesicles. Probably, a decrease of membrane curvature reduces the quantity of water molecules penetrated into the region of hydrocarbon

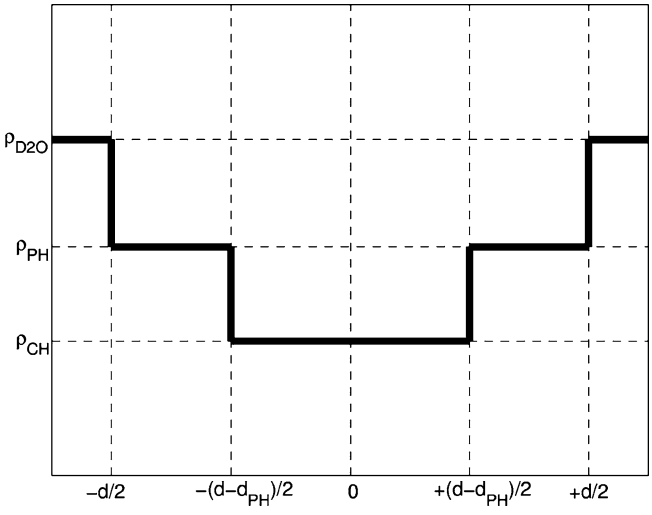

Fig. 10 Step function (SF) approximation of the neutron scattering length density across the lipid bilayer $\rho(x)$ with fixed thickness of the polar head group. d is the membrane thickness and $d_{PH} = 9$ Å is the thickness of the polar head group. ρ_{PH} is the scattering length density in the region of the polar head group

chains. But more precise experiments and data are necessary to check this. Surface area A calculated based on the SF approximation has an average value of 58 ± 1 Å^2, which is a little bit smaller than the value of 59.6 Å^2 for giant MLVs (Nagle and Tristram-Nagle 2000). The values of χ^2 for 500 Å extruded vesicles in L_α phase show that the HH approximation (Table 3) describes the membrane structure better relative to the SF approximation (Table 4).

DMPC vesicles in the $L_{\beta'}$ and the $P_{\beta'}$ phases, the SF approximation of $\rho(x)$

Figure 11 shows the SANS spectra from 500 Å extruded vesicles measured at $T = 10$°C ($L_{\beta'}$ phase) and $T = 30$°C (L_α phase). Without consideration of the vesicles polydispersity and the instrument resolution, the first minimum of $F_s(q, d)$ corresponds to $q_R = \pi/R$. The vesicle radius $R = 275.6$ Å corresponds to the $q_R = 0.011$ Å^{-1}. Shift of the q_R to larger values of q reflects the decrease of average vesicle radius at temperature lowering as seen from Fig. 11.

The consideration of SANS curves in the Guinier region of q from 0.03 to 0.14 Å^{-1} shows the different exponents at $T = 10$°C and $T = 30$°C (3). It is visually seen that at temperature decreasing from 30 to 10°C the radius of gyration of the bilayer R_t increases. This simple analysis corresponds to the dependence of the membrane thickness parameter d_G on temperature as shown in Fig. 2.

The application of the HH approximation for fitting SANS curve in $L_{\beta'}$ and $P_{\beta'}$ phases gives unreasonable results for bilayer structure. The basis of the HH approximation is the larger scattering length density of D_2O molecules inside the bilayer relative to that of polar head groups. It is true for L_α phase of DMPC. A common property of phospholipids is a decrease of hydration under phase transitions from L_α to $L_{\beta'}$ phases (Nagle and Tristram-Nagle 2000). We have every reason to consider other approximations of $\rho(x)$ for $L_{\beta'}$ and $P_{\beta'}$ phases. Different approximations have been tested to fit the experimental curve. The SF approximation of $\rho(x)$ with fixed thickness of the polar head region d_{PH} was selected as more appropriate for $L_{\beta'}$ and $P_{\beta'}$ phases of the DMPC bilayer (Fig. 10). A value of $\rho_{CH} = -0.396 \times 10^{10}$ cm^{-2} was used as fixed parameter in the calculations of $L_{\beta'}$ and $P_{\beta'}$ phases of DMPC. This value of ρ_{CH} reflects a decrease in the specific volume of the hydrocarbon chains from 781 Å^3 in the L_α phase to 710 Å^3 in the $L_{\beta'}$ phase (Nagle and Tristram-Nagle 2000; Tristram-Nagle et al. 2002). The structure of hydrocarbon chains in $L_{\beta'}$ and $P_{\beta'}$ phases is similar; no exact volumetric data exist for the $P_{\beta'}$ phase (Ruocco and Shipley 1982). The same value of ρ_{CH} was used in $L_{\beta'}$ and $P_{\beta'}$ phases.

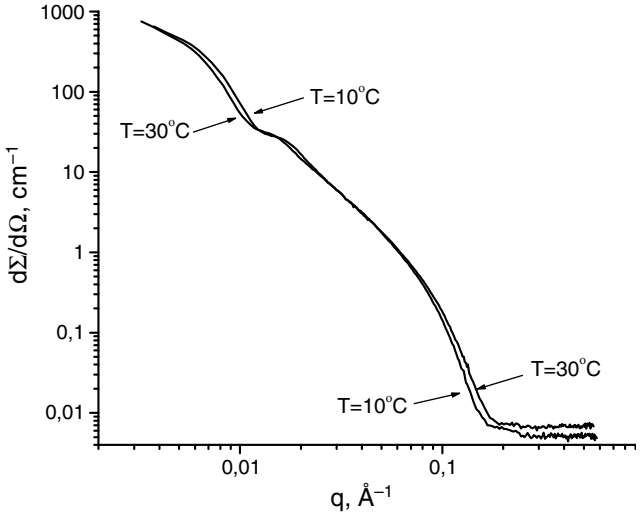

Fig. 11 Experimental macroscopic cross-sections of the ULVs populations at $T = 30$°C and $T = 10$°C for vesicles prepared by extrusion through pores of 500 Å diameter

Measured SANS curves of the $L_{\beta'}$ and the $P_{\beta'}$ phases for 500 and 1,000 Å extruded vesicles were fitted based on the SF approximation of $\rho(x)$. A deformation of the spherical shape to elliptical was taken into account. Unlike in the L_α phase, extruded 500 Å vesicles in $L_{\beta'}$ and $P_{\beta'}$ phases have pronounced elliptical form with eccentricity $\varepsilon = 1.6$. The 1,000 Å extruded vesicles have $\varepsilon = 1.1$ and can be considered as spherical taking into account problems in the determination of vesicle radius. The internal membrane structure did not show the dependence on the eccentricity and membrane curvature for both vesicle populations. The results of fitting and calculation are given in Table 4. The average values of the minor semi-axis $a = 185$ Å and the major semi-axis $b = 300$ Å in the $L_{\beta'}$ phase change to $a = 187$ Å and $b = 303$ Å in the $P_{\beta'}$ phase for 500 Å extruded vesicles. These values are in concurrence with the radius of pores. Similar to the L_α phase, the average radius of 1,000 Å extruded vesicles is underestimated relative to the radius of pores and DLS results. The DLS data is introduced to Table 4 for vesicle radius. Polydispersity of vesicle population has smaller values in $L_{\beta'}$ and $P_{\beta'}$ phases relative to that in the L_α phase. For 500 Å extruded vesicles, the polydispersity increases from the value of 21% in $L_{\beta'}$ phase to 26% in L_α phase. The average surface area of the 500 Å extruded vesicles $S = 4\pi\varepsilon a^2$ is equal to 9.9×10^5 Å^2 in the L_α phase. The average area of the vesicle decreases to the value of 7.2×10^5 Å^2 in the $P_{\beta'}$ and 7.0×10^5 Å^2 in the $L_{\beta'}$ phases. The decrease of vesicle area during the phase transitions from L_α to $L_{\beta'}$ phase should increase the membrane thickness. Membrane thickness increases from 47.8 ± 0.2 Å in the L_α phase to 49.1 ± 0.7 Å in the $L_{\beta'}$ phase.

Unlike in the L_α phase, the difference in the membrane curvature for 500 and 1,000 Å extruded vesicles has no influence on the membrane thickness and hydration in $L_{\beta'}$ and $P_{\beta'}$ phases. Values of the membrane thickness $d = 49.6 \pm 0.5$ Å and the surface area $A = 49.2 \pm 0.9$ Å^2 for 1,000 Å extruded vesicles are slightly larger than values $d = 48.2$ Å and $A = 47$ Å^2 determined for giant multilamellar DMPC vesicles in the

$L_{\beta'}$ phase hydrated by H_2O (Tristram-Nagleet al. 2002). Giant multilamellar DMPC vesicles can be considered as membrane with zero curvature. For the $L_{\beta'}$ phase, the number of D_2O molecules in the region of polar head groups per DMPC molecule $N_{w,PH}$ obtained for 500 and 1,000 Å extruded vesicles are the same. Average value of $N_{w,PH} = 5.6 \pm 0.5$ obtained in the $L_{\beta'}$ phase is smaller than hydration of the L_α phase, $N_{w,PH} = 7.4 \pm 0.6$.

Unlike in the L_α and $L_{\beta'}$ phases of DMPC, precise information about internal membrane structure and hydration in the $P_{\beta'}$ phase is hard to evaluate through the X-ray diffraction experiment due to the two dimensional lattice structure of the ripple bilayer. The ripple 141.7 Å profile of DMPC has the basic asymmetric triangular shape with the ripple amplitude of about 19 Å and the projection of the major ripple side on the lateral direction about 103 Å. Evaluation of electron density profiles along the normal to the major and minor sides (based on three diffraction orders) shows that internal bilayer structure is near to the $L_{\beta'}$ and L_α phases for major and minor sides, respectively (Sun et al. 1996). Further SAXS and WAXS investigations of $P_{\beta'}$ phase formation under T-jump protocol confirm that equilibrium bilayer structure of the $P_{\beta'}$ phase corresponds to the $L_{\beta'}$ phase with small percentage of the L_α phase. Probably, bilayer in the L_α phase exists in the corners of triangular ripple (Rappolt et al. 2000).

The used SANS evaluation of bilayer structure cannot make out the coexistence of two phases in the $P_{\beta'}$ phase. The data evaluated from SANS correspond to the average bilayer parameters. Parameters of the vesicle population and the bilayer structure of DMPC vesicles in ripple phase are given in Table 4. For 500 Å extruded vesicles, the evaluated vesicle parameters are the same in $L_{\beta'}$ and $P_{\beta'}$ phases within the range of experimental errors. For 1,000 Å extruded vesicles, the membrane thickness decreases from the value of 49.6 ± 0.5 Å in the $L_{\beta'}$ phase to 48.3 ± 0.6 Å in the $P_{\beta'}$ phase. This 1.3 Å decrease in the membrane thickness could be explained by the coexistence of $L_{\beta'}$ and L_α phases in the bilayer of the $P_{\beta'}$ phase. Finally, one can use parameters evaluated for 1,000 Å extruded vesicles $d = 48.3 \pm 0.6$ Å, $N_{w,PH} = 5.9 \pm 0.4$ and $A = 50.4 \pm 0.8$ Å to characterize the average DMPC bilayer structure in the $P_{\beta'}$ phase.

Guinier approximation for the flat membrane, connection with SFF model

It is commonly believed that the Guinier approximation describes the SANS curve at $q \to 0$. This is true for globular particles with one typical size (Guinier and Fournet 1955). ULVs have two typical sizes: radius and membrane thickness, which are different in the scale of 1–2 orders of magnitude. SANS curves from vesicles have two Guinier regions. The first Guinier region is that of the vesicle size at $q \to 0$ and the other is the Guinier region of the membrane. The utility and validity of the membrane Guinier approximation is clarified below.

Let one consider a lipid membrane as that with $\rho_c(x) \equiv \Delta\rho = \text{const}$. This approximation is conventionally named the homogenous approximation (Feigin and Svergun 1987). Really, a lipid membrane is non-homogenous, $\rho_c(x) \neq \text{const}$. The homogenous approximation can describe only some part of the experimental scattering curve (Feigin and Svergun 1987). This part of the curve can be obtained via comparison of experimental and calculated SANS curves (Kiselev et al. 2002). The homogeneous region of SANS curve is limited by $q \approx 0.16$–0.17 Å^{-1} for the L_α phase of DMPC. According to the SFF model, the scattering amplitude of vesicles for $\rho_c(x) \equiv \Delta\rho = \text{const}$ and $R >> d_G$ is written as (Kiselev et al. 2002)

$$A(q) = \left(4\pi R^2 \frac{\sin(qR)}{qR}\right)\left(\frac{2\Delta\rho}{q}\sin\left(\frac{qd_G}{2}\right)\right). \quad (24)$$

The approximation of the harmonic function by exponent

$$\frac{\sin x}{x} \approx \exp\left(-\left(\frac{x}{\sqrt{6}}\right)^2\right) \quad (25)$$

is valid for $x < 1$. Equation (24) can be rewritten as

$$A(q) = \left(S\frac{\sin(qR)}{qR}\right)\Delta\rho d_G \exp\left(-\frac{(qd_G)^2}{24}\right), \quad (26)$$

where $S = 4\pi R^2$ is the vesicle surface area. It is important to note that transition from the harmonic function to the exponent has no request of $q \to 0$. The validity of this transformation is $q(d_G/2)$ The exponential presentation of the scattering amplitude is the principal property of the Guinier approximation. For q the vesicle form factor $F = A^2$ is written as

$$F(q) = \left(\frac{4\pi S \sin^2(qR)}{q^2}\right)(\Delta\rho d_G)^2 \exp\left(-\frac{(qd_G)^2}{12}\right). \quad (27)$$

Let us consider a flat lipid bilayer, which corresponds to $R \to \infty$. In this case, $\Delta q = (\pi/R) \to 0$, where Δq is the distance between minima of the $\sin^2(qR)$. Any SANS spectrometer has uncertainty in the measured values of q, also as any vesicle population has uncertainty in the value of R. One can, therefore, use the average value $\sin^2(qR) = 1/2$ instead of $\sin^2(qR)$. Finally, using (4) for R_t, one obtains

$$F(q) = \left(\frac{2\pi S}{q^2}\right)(\Delta\rho d_G)^2 \exp\left(-q^2R_t^2\right). \quad (28)$$

Equation (28) is the Guinier approximation of the form factor for the flat bilayer with infinitely large area S and membrane radius of gyration R_t. The form factor of the infinitely thin flat membrane has $1/q^2$ behavior. The form factor of the membrane with thickness parameter d_G has exponential form and is characterized at $q \to 0$ by asymptotic properties of the function $F(q)q^2$. Equation (28) was evaluated from the SFF model on the basis

of two approximations: $\Delta\rho = \text{const}$ and $R \to \infty$. According to the above analytical analysis, only one membrane parameter d_G can be evaluated from SANS curve in the region of Guinier, which is the region of homogeneous approximation. Unhomogeneous structure of the membrane corresponds to the next region of scattering curve $q > (2/d_G)$.

Dependence of the membrane thickness parameter d_G on temperature as shown in Fig. 2 can be corrected now for the values of membrane thickness calculated for 1,000 Å extruded vesicles at 10, 20 and 30°C. Obtained values of parameter Δd_H are 5.4, 4.9 and 6.7 Å, respectively, for the $L_{\beta'}$, $P_{\beta'}$ and L_α phases of DMPC. Membrane thickness d is calculated using (5) with an assumption that Δd_H has permanent values in the $L_{\beta'}$, $P_{\beta'}$ and L_α phases. Figure 12 shows the obtained dependence of the DMPC membrane thickness on temperature for 1,000 Å extruded vesicles. The main feature in temperature dependence $d(T)$ is a sharp increase in the membrane thickness at the temperature of the main phase transition $T = 23.8$°C.

Structure of the DMPC bilayer

The important question to be emphasized is what is the meaning of the obtained membrane parameters d and D and, correspondingly, what is the meaning of their accuracy. In SANS we cannot measure directly the steric thickness of the membrane or of the hydrophobic core. The evaluated information from SANS are parameters of the neutron scattering length density distribution function $\rho(x)$ and, correspondingly, the experimental errors presented in Tables 3 and 4 are related to the accuracy of the function parameters. High accuracy of the obtained parameters demonstrates a stable convergence of the fitting curve to the experimental.

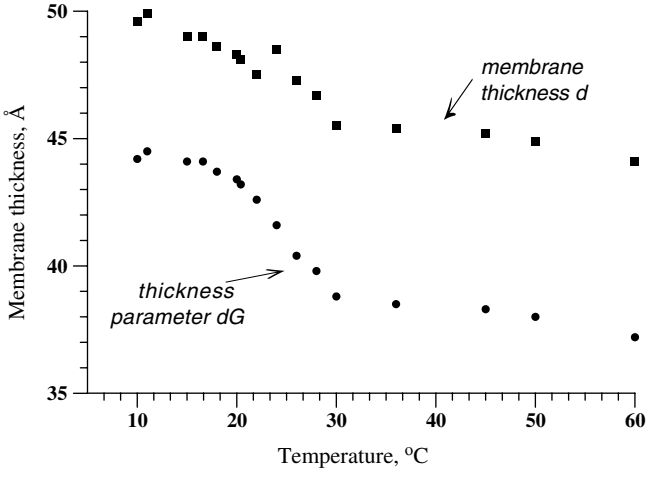

Fig. 12 Dependence of DMPC membrane thickness parameter d_G and membrane thickness d on temperature for 1,000 Å extruded vesicles

From numerical results obtained with the HH approximation for spherical and elliptical vesicle forms, one can conclude that the accuracy of the membrane thickness evaluation is about 1 Å. This value of accuracy characterizes the accuracy of the SANS method. HH and SF approximations of the $\rho(x)$ describe only the main features of the $\rho(x)$ function. For DMPC in L_α phase, the $\rho(x)$ function based on Gaussian approximation was evaluated from SANS experiment on the DMPC vesicles (Kiselev et al. 2004). For the L_α phase of DPPC hydrated by D_2O, the $\rho(x)$ function was calculated via dynamic simulations (Kucerka et al. 2004c). Presented results show that the HH approximation describes the neutron scattering length density better than the SF approximation. Similar conclusions were made via application of HH and SF approximations for the fitting of SANS curves of POPC oligolamellar vesicles with different membrane curvatures (Schmiedel et al. 2005). Biological membrane has a negligible curvature. Thus, results obtained by HH approximation for 1,000 Å extruded vesicles in the L_α phase are more biologically relevant. It is important to compare these results with results obtained by other methods. DMPC bilayer parameters evaluated from the complementary application of the X-ray diffraction on the oriented sample and SAXS on the extruded ULVs are: $d = 43.4$ Å, $A = 60.6$ Å^2 and $N_{w,PH} = 7.2$ (Kucerka et al. 2005). These results are different from the presented $d = 45.5 \pm 0.6$ Å, $A = 62.6 \pm 1.0$ Å^2 and $N_{w,PH} = 8.0 \pm 0.6$.

The second important question is water penetration depth into the lipid bilayer. For many decades it was a common opinion that water penetrates only into the polar head group region. Recently, water penetration into the region of hydrocarbon chains was detected experimentally for saturated phospholipids by nuclear magnetic resonance (Tokutake et al. 2004), SANS (Schmiedel et al. 2001, 2005; Kiselev et al. 2004) and neutron diffraction (Kiselev et al. 2005b). Presented SANS results support the water penetration into the region of hydrocarbon chains. Thickness of the DMPC hydrophilic part $D_H = (d - D/2) = 12.4 \pm 0.5$ Å is calculated from obtained value of $d = 45.5 \pm 0.5$ Å and $D = 20.8 \pm 0.4$ Å in the L_α phase. The value of D_H is larger than the thickness of the polar head group $D_{PH} = 9$ Å, evaluated from X-ray diffraction (Nagle and Tristram-Nagle 2000). Consequently for DMPC, water molecules penetrate into the hydrocarbon chain region at 3.4 Å. Finally, water penetration into the region of hydrocarbon chains of saturated phospholipids can be estimated as about 3 Å. About hydration of the polar head region, the obtained value $N_{w,PH} = 8.0 \pm 0.6$ can characterize the number of D_2O molecules in the polar head group of DMPC at 30°C.

The structure of lipid bilayer hydrated by D_2O in the $L_{\beta'}$ phase is characterized by $d = 49.6 \pm 0.5$ Å, $A = 49.2 \pm 0.9$ Å^2 and $N_{w,PH} = 5.6 \pm 0.5$. Averaged over two component phases, the structure of the lipid bilayer in the $P_{\beta'}$ phase is characterized by $d = 48.3 \pm 0.6$ Å, $A = 50.4 \pm 0.8$ Å^2 and $N_{w,PH} = 5.9 \pm 0.4$.

Membrane thickness 45.5 Å in the L_α and 49.6 Å in the $L_{\beta'}$ phases of extruded vesicles in D_2O is larger than the relative corresponding values of 43.4 and 48.2 Å evaluated from MLVs hydrated by H_2O. Two reasons could be the source of this difference. The first reason is the non-equilibrium structure of extruded vesicles and the dependence of the bilayer parameters on membrane curvature. DMPC bilayer is stressed after extrusion and extruded vesicles aggregate into MLVs. The second reason could be the difference in the bilayer structure hydrated by D_2O and H_2O. Strengths of hydrogen and deuterium bonds are different (Matsuki et al. 2005). X-ray diffraction study shows no difference in the repeat distances of the DMPC hydrated by H_2O or D_2O in $L_{\beta'}$ and $P_{\beta'}$ phases, whereas the repeat distance of L_α phase in D_2O is about 0.5 Å smaller relative to that in H_2O (Kobayashi and Fukado 1998). This experimental result is inconsistent with the presented 2.1 Å increase of DMPC membrane thickness in D_2O and demonstrates that the main component is the influence of the membrane curvature.

Conclusions

The separated form factor model of the small-angle scattering can be used for data interpretation for vesicles with a radius larger than 250 Å. The Shultz distribution describes well the vesicle shape and size for vesicles prepared via extrusion through pores of 500 Å. Average vesicle shape is near to spherical (eccentricity 1.1) for the L_α phase of DMPC and deviates sufficiently from the sphere in $L_{\beta'}$ and $P_{\beta'}$ phases (eccentricity 1.6). The approximation of the neutron scattering length density across the DMPC bilayer in the L_α phase as hydrophobic and hydrophilic regions with linear water distribution describes the internal bilayer structure without any preliminary structural information. The step function approximation of the scattering length density allows evaluation of the DMPC membrane thickness and neutron scattering length density of the polar head group in the $L_{\beta'}$, $P_{\beta'}$ and L_α phases based on the preliminary structural information about the thickness of the polar head group. The DMPC bilayer thickness of the curved ULVs after extrusion in D_2O (49.6 ± 0.5 and 45.5 ± 0.6 Å in $L_{\beta'}$ and L_α phases, respectively) is larger relative to that of the flat membrane (48.2 and 43.4 Å in $L_{\beta'}$ and L_α phases, respectively). Information about the specific volume of the lipid molecule allows one to receive additional structural information from SANS. A preliminary knowledge of the DMPC molecular volume allows one to calculate bilayer hydration and lipid surface area. Average structure of lipid bilayer in the $P_{\beta'}$ phase is characterized by $d = 48.3 \pm 0.6$ Å, $A = 50.4 \pm 0.8$ Å and $N_{w,PH} = 5.9 \pm 0.4$.

The results presented here emphasize the importance of appropriate models and approximations for the interpretation of SANS data. The usefulness of SANS technique for the characterization of the internal bilayer structure and hydration was described for vesicular systems. Development of flexible vesicles for penetration through human skin is one from perspective nanotechnologies of the drug delivery systems (Cevc et al. 2002). The methods discussed herein can be used for the characterization of such vesicular systems during their formulation.

Acknowledgements This work is partly based on the experiments performed at Swiss spallation neutron source SINQ, Paul Scherrer Institute, Villigen, Switzerland. The authors are grateful to V.L. Aksenov for his support, H. Schmiedel and A.M. Balagurov for fruitful discussions and K. Schwarz for performing DSC measurements. The investigation was supported by Grant of Leading Scientific Scholl, Grant of the Federal State of Saxony-Anhalt (project no. 3482A/1102L) and RFBR (grant no. 03-01-00657). The authors would like to thank Lipoid (Moscow) for the gift of DMPC.

References

Armen PS, Uitto OD, Feller SE (1998) Phospholipid component volumes: determination and application to bilayer structure calculations. Biophys J 75:734–744

Balgavy P, Dubnickova M, Uhrikova D, Yaradaikin S, Kiselev M, Gordeliy V (1998) Bilayer thickness in unilamellar extruded egg yolk phosphatidylcholine liposomes: a small-angle neutron scattering study. Acta Phys Slovaca 48:509–533

Balgavy P, Dubnickova M, Kucerka N, Kiselev MA, Yaradaikin SP, Uhrikova D (2001) Bilayer thickness and lipid interface area in unilamellar extruded 1,2-diacylphosphatidylcholine liposomes: a small-angle neutron scattering study. Biochim Biophys Acta 1521:40–52

Cevc G, Schatzlein A, Richardsen H (2002) Ultradiformable lipid vesicles can penetrate the skin and other semi-permiable barriers unfragmented. Evidence from double label SLSM experiments and direct size measurements. Biochim Biophys Acta 1564:21–30

Dymov SN, Kurbatov VS, Silin IN, Yaschenko SV (2000) Constrained minimization in C++ environment. Nucl Instrum Methods Phys Res A 440:431–437

Eadie WT, Dryan D (1971) Statistical methods in experimental physics. North-Holland, Netherlands

Feigin LA, Svergun DI (1987) Structure analysis by small-angle X-ray and neutron scattering. Plenum, New York

Glatter O (1977) Data evaluation in small angle scattering: calculation of the radial electron density distribution by means of indirect Fourier transformation. Acta Phys Austriaca 47:83–102

Glatter O (1980) Evaluation of small-angle scattering data from lamellar and cylindrical particles by the indirect transformation method. J Appl Crystallogr 13:577–584

Gordeliy VI, Kiselev MA (1995) Definition of lipid membrane structural parameters from neutronographic experiments with the help of the strip function model. Biophys J 69:1424–1428

Gordeliy VI, Golubchikova LV, Kuklin AI, Syrykh AG, Watts A (1993) The study of single biological and model membranes via small angle neutron scattering. Prog Colloid Polym Sci 92:252–257

Gordeliy VI, Cherezov V, Teixeira J (2005) Strength of thermal undulations of phospholipid membranes. Phys Rev E 72:061913

Guinier A, Fournet G (1955) Small-angle scattering of X-rays. Wiley, New York

Hallet FR, Watton J, Krygsman P (1991) Vesicle sizing. Number distributions by dynamic light scattering. Biophys J 59:357–362

Ibel K, Stuhrmann HB (1975) Comparison of neutron and x-ray scattering of dilute myoglobin solutions. J Mol Biol 93:255–265

Jin AJ, Huster D, Gawrisch K, Nossal R (1999) Light scattering characterization of extruded lipid vesicles. Eur Biophys J 28:187–199

Kiselev MA, Lesieur P, Kisselev AM, Lombardo D, Killany M, Lesieur S (2001) Sucrose solutions as prospective medium to study the vesicle structure: SAXS and SANS study. J Alloys Compd 328:71–76

Kiselev MA, Lesieur P, Kisselev AM, Lombardo D, Aksenov VL (2002) Model of separated form factors for unilamellar vesicles. J Appl Phys A 74(Suppl):S1654–S1656

Kiselev MA, Lombardo D, Kisselev AM, Lesieur P, Aksenov VL (2003a) Structure factor of dimyristoylphosphatidylcholine unilamellar vesicles: small-angle X-ray scattering study (in Russian). Surf X-Ray Synchrotron Neutron Res 11:20–24

Kiselev MA, Wartewig S, Janich M, Lesieur P, Kiselev AM, Olli-von M, Neubert R (2003b) Does sucrose influence the properties of DMPC vesicles? Chem Phys Lipids 123:31–44

Kiselev MA, Zemlyanaya EV, Aswal VK (2004) SANS study of unilamellar DMPC vesicles: fluctuation model of a lipid bilayer. Crystallogr Rep 49(Suppl 1):s136–s141

Kiselev MA, Zbytovska J, Matveev D, Wartewig S, Gapienko IV, Perez J, Lesieur P, Hoell A, Neubert R (2005a) Influence of trehalose on the structure of unilamellar DMPC vesicles. J Colloid Surf A Physicochem Eng Aspects 256:1–7

Kiselev MA, Ryabova NY, Balagurov AM, Dante S, Hauss T, Zbytovska J, Wartewig S, Neubert RHH (2005b) New insights into structure and hydration of stratum corneum lipid model membrane by neutron diffraction. Eur Biophys J 34:1030–1040

Knoll W, Haas J, Stuhrmann H, Fuldner HH, Vogel H, Sackmann E (1981) Small-angle neutron scattering of aqueous dispersions of lipids and lipid mixtures A contrast variation study. J Appl Crystallogr 14:191–202

Kobayashi Y, Fukado K (1998) The lamellar repeat distance of phospholipid bilayers in excess H_2O and D_2O. A small-angle X-ray scattering study. Chem Lett:1105–1106

Korgel B, van Zanten JH, Monbouquette HG (1998) Vesicle size distributions measured by flow field-flow fractionation. Biophys J 74:3264–3272

Kucerka N, Uhrikova D, Teixeira J, Balgavy P (2004a) Bilayer thickness in unilamellar phosphatidylcholine vesicles: small-angle neutron scattering using contrast variation. Physica B 350:e639–e642

Kucerka N, Kiselev MA, Balgavy P (2004b) Determination of bilayer thickness and lipid surface area in unilamellar dimyristoylphosphatidylcholine vesicles from small-angle neutron scattering curves: a comparison of evaluation methods. Eur Biophys J 33:328–334

Kucerka N, Nagle JF, Feller SF, Balgavy P (2004c) Models to analyze small-angle neutron scattering from unilamellar lipid vesicles. Phys Rev E 69:051903

Kucerka N, Liu Y, Chu N, Petrache HI, Tristram-Nagle S, Nagle JF (2005) Structure of fully hydrated fluid phase DMPC and DLPC lipid bilayers using X-ray scattering from oriented multilamellar arrays and from unilamellar vesicles. Biophys J 88:2626–2637

MacDonald RC, MacDonald RI, Menco BP, Takeshita K, Subbarao NK, Hu LR (1991) Small-volume extrusion apparatus for preparation of large, unilamellar vesicles. Biochim Biophys Acta 1061:297–303

Matsuki H, Okuno H, Sakano F, Kusube M, Kaneshina S (2005) Effect of deuterium oxide on the thermodynamic quantities associated with phase transitions of phosphatidylcholine bilayer membranes. Biochim Biophys Acta 1712:92–100

Nagayasu A, Uchiyama K, Kiwada H (1999) The size of liposomes: a factor which affects their targeting efficiency to tumors and therapeutics activity of liposomal antitumor drugs. Adv Drug Deliv Rev 40:75–87

Nagle JF, Tristram-Nagle S (2000) Structure of lipid bilayers. Biochim Biophys Acta 1469:159–195

Ostanevich YuM (1988) Time-of-flight small-angle scattering spectrometers on pulsed neutron sources. Macromol Chem Macromol Symp 15:91–103

Patty PJ, Frisken BJ (2003) The pressure-dependence of the size of extruded vesicles. Biophys J 85:996–1004

Pedersen JS, Posselt D, Mortensen K (1990) Analytical treatment of the resolution function for small-angle scattering. J Appl Crystallogr 23:321–333

Pencer J, Hallet R (2000) Small-angle neutron scattering from large unilamellar vesicles: an improved method for membrane thickness determination. Phys Rev E 61:3003–3008

Pencer J, White GF, Hallet FR (2001) Osmotically induced shape changes of large unilamellar vesicles measured by dynamic light scattering. Biophys J 81:2716–2728

Rappolt M, Pabst G, Rapp G, Kriechbaum M, Amenitsch H, Krenn C, Bernstorff S, Laggner P (2000) New evidence for gel–liquid crystalline phase coexistence in the ripple phase of phosphatidylcholines. Eur Biophys J 29:125–133

Ruocco MJ, Shipley GG (1982) Characterization of the sub-transitions of hydrated dipalmitoylphosphatidylcholine bilayers. Kinetics, hydration and structural study. Biochim Biophys Acta 691:309–320

Schalke M, Kruger P, Weygand M, Losche M (2000) Submolecular organization of DMPA in surface monolayers: beyond the two-layer model. Biochim Biophys Acta 1464:113–126

Schmiedel H, Joerchel P, Kiselev M, Klose G (2001) Determination of structural parameters and hydration of unilamellar POPC/C12E4 vesicles at high water excess from neutron scattering curves using a novel method of evaluation. J Phys Chem B 105:111–117

Schmiedel H, Almasy L, Klose G (2005) Multilamellarity, structure and hydration of extruded POPC vesicles by SANS. Eur Biophys J:s00249-005-0015-9, online first

Sun WJ, Tristram-Nagle S, Suter RM, Nagle JF (1996) Structure of the ripple phase in lecithin bilayers. Proc Natl Acad Sci USA 93:7008–7012

Tokutake N, Jing B, Regen SL (2004) Probing the hydration of lipid bilayers using a solvent isotope effect on phospholipid mixing. Langmuir 20:8958–8960

Tristram-Nagle S, Liu Y, Legleiter J, Nagle JF (2002) Structure of gel phase DMPC determined by X-ray diffraction. Biophys J 83:3324–3335

Weiss TM, Narayanan T, Wolf C, Gradzielski M, Panine P, Finet S, Helsby WI (2005) Dynamics of the self-assembly of unilamellar vesicles. Phys Rev Lett 94:038303

Wiener MC, White SH (1991) Fluid bilayer structure determination by the combined use of X-ray and neutron diffraction. Biophys J 59:162–173